We thank the referees for their careful reading of the manuscript and helpful comments, which are repeated below (in black font). Our replies are given in blue font directly after each comment.

Referee 1:

General comments

Time-resolved experiments have been carried out to generate two Criegee: CH_2OO, which has been study many times; and MVKOO, which has only very recently been studied. In the presence of dimethyl sulphide, no additional Criegee removal was evident. Hence, only an upper limit is assigned for the rate coefficients. A theoretical potential energy surface has been calculated for CH2OO + (CH3)2S that has a significant barrier to products (DMSO + CH_2O) and its rate coefficient is lower than the experimental upper limit. These results are clear-cut and only a few specific comments are raised.

If this were the only study on the titled reaction, the lack of reactivity would probably mean this paper would not be considered for publication in ACP. The reason this result is significant is that a previous study (Newland 2015) suggested the stabilized Criegee formed from O_3/isoprene (mainly CH_2OO/MKVO) react rapidly with dimethyl sulphide, with a rate coefficient close to the gas-kinetic frequency. As this other study generated the Criegees via ozonolysis (O_3/isoprene), it does ask the question how we best understand ozonolysis in the atmosphere. Is stabilized Criegee chemistry the most important component of ozonolysis? More detail would help this paper. The comment from Andrew Rickard expands on this.

Specific comments

Line 39 "*Surprisingly, the obtained rate coefficients are up to 10^4 times larger than previous results deduced from ozonolysis experiments, indicating that the ozonolysis experiments could be quite complicated such that reliable kinetic results may be hard to retrieve.*"

This needs a reference. This is interesting in that relative rate experiments appear to be out by orders of magnitude. Is there explanation of these studies with today's knowledge? Is it wrong rate coefficients or is it more to do with the experiment itself?

AUTHORS' REPLY:

Welz et al. (2012) compared their rate coefficients with previous values applied in contemporary tropospheric models (Johnson and Marston, 2008; Johnson et al., 2001; Hatakeyama and Akimoto, 1994). For ozonolysis experiments, typically only the ratios of reaction rate coefficients, e.g. k_{DMS}/k_{SO2} (Newland et al., 2015), are obtained. The researchers have to compare with (at least) one absolute rate coefficient to get the rest rate coefficients. Unfortunately, the selected absolute rate coefficient (at that time) has large uncertainty, which propagates to other reported values. In addition, the reaction mechanism may be rather complicated and even the ratios of the rate coefficients must be treated with care. The above three references will be included in the main text.

Line 103 "*To compensate for this effect, which was caused by the optics and the photolysis laser pulse, we recorded background traces without adding the precursor before and after each set of experiments. The reported data are after background subtraction.*" Can you state the typically size of this signal, i.e. what is I/I0 in the absence of added chemicals. Is it related to a heating effect?

AUTHORS' REPLY:

Typical background traces as well as raw signal traces (without background subtraction) obtained at 248 nm and 308 nm will be shown in Figures S5 and S6, respectively. These backgrounds are originated from the different longpass filters used for coupling the laser beam and probe beam into the reactor. Yes, it is likely that the backgrounds are from a heating effect of the longpass filters.

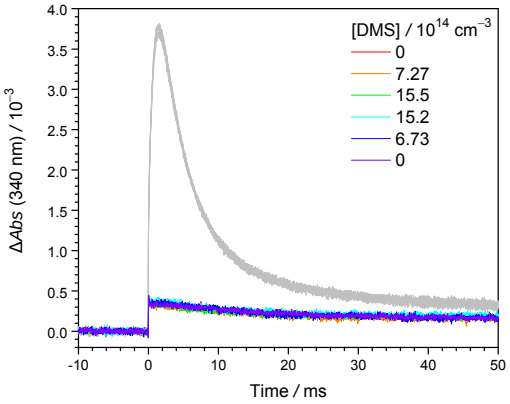

Fig. S5. Background traces under normal DMS concentrations, represented in colour lines, and the raw signal traces (without background subtraction), represented in grey lines, obtained with 248 nm photolysis laser (I_{248nm} = 2.43 mJ cm^{-2}). See Exp#22 of Table S3 for the experimental conditions.

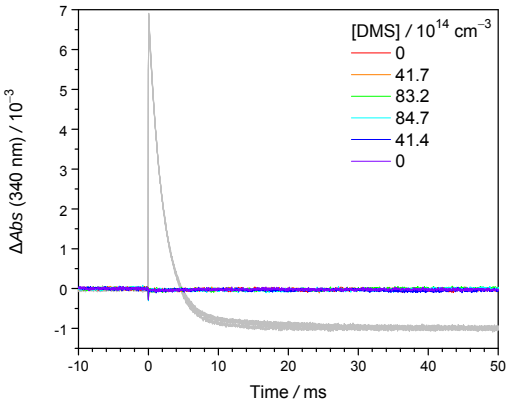

Fig. S6. Background traces under normal DMS concentrations, represented in colour lines, and the raw signal traces (without background subtraction), represented in grey lines, obtained with 308 nm photolysis laser (I_{308nm} = 2.35 mJ cm^{-2}). See Exp#2 of Table S1 for the experimental condition. Note that the optics (longpass filters) are different from those at 248 nm.

Line 134 "*e.g., bimolecular reactions with radical byproducts like I atoms, wall loss, etc.*" Probably self-reaction is most important. Any evidence for a second-order component?

This paper has probably done most to unravel the removal the kinetics in absence of added

reagent. CH2OO Criegee intermediate UV absorption cross-sections and kinetics of CH2OO + CH2OO and CH2OO + I as a function of pressure By:Mir, ZS (Mir, Zara S.)[1] ; Lewis, TR (Lewis, Thomas R.)[1] ; Onel, L (Onel, Lavinia)[1] ; Blitz, MA (Blitz, Mark A.)[1,2] ; Seakins, PW (Seakins, Paul W.)[1] ; Stone, D (Stone, Daniel)[1]

AUTHORS' REPLY:

In the previous works of Smith et al. (Smith et al., 2016) and Li et al. (Li et al., 2020), the contributions of the pseudo-first-order reactions and second-order reactions are both considered and the kinetic model can be represented in the following equation:

$$\frac{-d[\mathrm{CI}]}{dt} = k_1[\mathrm{CI}] + k_2[\mathrm{CI}]^2$$

The above equation can be simplified when extrapolating the rate coefficients to zero concentration of $[CI]_0$:

$$\frac{-d[\mathrm{CI}]}{dt} \cong (k_1 + \frac{1}{2}k_2[\mathrm{CI}]_0)[\mathrm{CI}] = k_{\mathrm{obs}}[\mathrm{CI}]$$

The difference between the complete and simplified equations only shows up at high $[CI]_0$. Most important of all, the self-reaction of CIs would not affect the determination of k_{DMS}, since $[CI]_0$ was kept constant in every experimental set.

Based on the absolute absorption cross section of CH_2OO at 340 nm (σ = 1.23×10^{-17} cm^2) and the pressure-dependent yield of CH_2OO from $CH_2I + O_2$ (0.46 at 300 Torr) (Ting et al., 2014a) the number densities of relevant species can be estimated to be the following (for Exp#1, Table S1).

$[CH_2OO]_0 = 6.7\times10^{11}$ cm^{-3}; $[I]_0 = 2.1\times10^{12}$ cm^{-3}; $[CH_2IOO]_0 = 7.7\times10^{11}$ cm^{-3}.

The first-order decay rate coefficient of CH_2OO (k_{eff}) can be approximately estimated (Li et al., 2020) as:

$$k_{\mathrm{eff}} = k_{\mathrm{I}}[\mathrm{I}]_0 + k_{\mathrm{self}}[\mathrm{CH_2OO}]_0$$

Using k_{self} = 8×10^{-11} cm^3 s^{-1} and k_I = 5.8×10^{-11} cm^3 s^{-1} at 300 Torr (Mir et al., 2020), the estimated k_{eff} is 180 s^{-1}, consistent with the observed value of 232 s^{-1} for k_0. Therefore, the main loss processes of CH_2OO are reaction with iodine atoms (and other radicals) and its self-reaction.

In Figure S7, we can see a nice linear relationship between k_0 and the total produced radicals (proportional to the product of the laser fluence and the precursor concentration), further supporting the above mechanism. We would add the following sentences in the caption of Figure S7.

"The main loss processes of CH_2OO are reactions with radical byproducts like iodine atoms and its self-reaction. The observed values of k_0 (e.g., 232 s^{-1} for Exp#1) are consistent with the values (e.g., 180 s^{-1} at the condition of Exp#1) that are estimated using the reported kinetic data (yield and rate coefficients) (Mir et al., 2020; Ting et al., 2014)."

We will also modify the relevant sentences in the main text to:

"*The subsequent decay in absorption is due to the consumption of CH_2OO either through reaction with DMS or through other processes, e.g., bimolecular reactions with radical byproducts like I atoms, wall loss, etc. In addition, self-reaction of CH_2OO has been found to be rather fast ($k_{self} = 8\times10^{-11} cm^3 s^{-1}$)(Mir et al., 2020). However, the effect of the self-reaction (Smith et al., 2016;Li et al., 2020) would not affect the determination of k_{DMS} under our experimental conditions.*"

Line 155 "*and show the results in Table S4.*" , From Table S4, the results given in Figure 2 are fairly obvious. I would expected a similar result even if 248 nm photolysis was used. Significant photolysis of DMS could potentially lead to enhanced reactivity, and an energy dependence would be good practice. However, in the present case, there is no evidence of enhanced Criegee removal so there is not too much to worry about.

AUTHORS' REPLY:

In Table S4, we have shown that $[DMS]_{diss}$ is about ten times less than $[CH_2I_2]_{diss}$ under typical experimental conditions when 248 nm photolysis is applied. However, we have observed a strong absorption in the background traces when 248 nm photolysis and high [DMS] are applied (Figure S4). The extra absorption from the dissociated DMS would be problematic when performing the background subtraction. Therefore we constrained the laser fluence and [DMS] to preclude the influence of [DMS] photolysis.

Line 171 "*See SI (Sect. S3, page S5) for details.*" From the SI (Table S3), the instant yield of MVKOO decreases with total pressure, which is consistent with population into $CH_3(C_2H_3)CIOO$, i.e. the SV is linear. However, k_r appears to be faster at low pressures. k_r is the rate coefficient for the peroxy radical to react to MVKOO + I. It is not possible for a rate coefficient to increase at lower total pressure. There are too few pressures to say anything for definite, but it does highlight that the k_r errors are not realistic.

I wonder if there is another explanation for the results in Table S3. If you had an additional species, produced from the photolysis of the di-iodo compound, X, that can react with the di-iodo compound to make the iodo radical.

$$\text{di-iodo} + hv \rightarrow X$$

$$X + \text{di-iodo} \rightarrow \text{iodo radical}$$

The pressure dependence could be linked to the fact the MVKOO species has a double bond.

If k_r is the unimolecular reaction $CH_3(C_2H_3)CIOO \rightarrow$ MVKOO + I, then changing the temperature should be the easiest way to identify it.

Line 172 "*This difference is consistent with the fact that MVKO is resonance-stabilized due to the extended conjugation of its vinyl group (Barber et al., 2018) and thus the adduct $CH_3(C_2H_3)CIOO$ is relatively less stable due to disruption of the conjugation.*"

It will be the properties of $CH_3(C_2H_3)CIOO$ that will most strongly influence its formation and unimolecular dissociation, k_r.

AUTHORS' REPLY (To lines 171-172):

The reviewer is right about the role of $CH_3(C_2H_3)CIOO$ and that changing the temperature should be the easiest way to identify the related process. In fact, we have discussed the issues of the adduct, including the temperature and pressure effects, in our recent paper (Lin et al., 2020). Since MVKO is a resonance-stabilized molecule, adduct would be relatively less stable, compared with CIs without resonance structure, such as CH_2OO or CH_3CHOO. Therefore, the unimolecular decomposition of the adduct is observed in our experimental time scale. The reason why k_r appears to be larger at lower pressure is that the fitted k_r should include the unimolecular decomposition of the adduct and the reaction of the adduct with other radicals (X) such as iodine atoms.

$$k_r = k_{uni}(\text{adduct}) + k_x[X]$$

The concentration of the radicals would increase as the precursor concentration increases, leading to a higher k_r. This relation can be observed explicitly through plotting k_r against $I_{248\ nm} \times Abs(238\ nm)$ (photolysis laser fluence times precursor absorbance). As for the temperature effect, we have also observed a positive temperature dependence of k_r (E_a = 12.7±0.3 kcal mol^{-1}), consistent with the calculation result for the bond dissociation energy of the adduct (14 kcal mol^{-1}) (Lin et al., 2020).

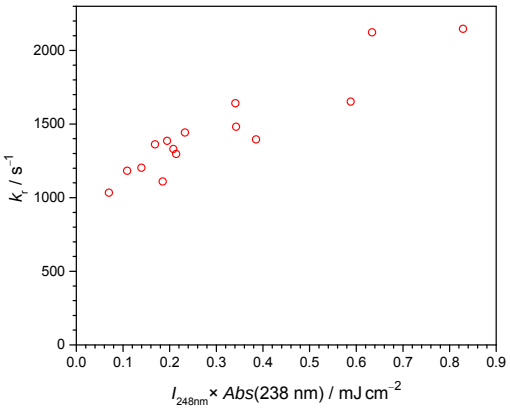

Fig. S?. Plot of k_r against the product of the laser fluence (I_{248nm}) and the absorbance of 1,3-diiodo-2-butene at 238 nm in the photolysis cell (Abs(238nm)) for the experiments of MVKO+DMS reaction (Exp#15-29, Tables S3). The x-axis essentially represents the total amounts of radical species generated through the photolysis of the precursor (R1) and the subsequent reactions (R2). Higher radical concentration results in faster decay of the adduct, thus higher k_r.

Please note that the error bars in Tables S1-S3 do NOT include any systematic errors. For k_r, it is correlated with other fitting parameters like (1−α). Since MVKO does not react with DMS (essentially all the traces are almost the same at various [DMS]), it is hard to 'disentangle' the correlation among fitting parameters. In the paper by Lin et al., we used SO_2 to scavenge MVKO and to obtain more robust results (Lin et al., 2020).

We will add a notation regarding the error bar of k_r after Table S3:

"*averaged value ± 1 sigma error of the mean (statistical only, not including systematic*

errors). The actual error bar would be larger since k_r is highly correlated with other fitting parameters like (1−α). Lin et al. has used SO_2 scavenger to obtain more robust results for k_r (Lin et al., 2020).”

Line 194 “*Here we choose the boundary of three standard deviations as the upper limits for k_{DMS}+CI, k_{DMS}+$CH_2OO \leq 4.2\times10^{15}$ cm^3s^{-1} and k_{DMS}+MVKO $\leq 1.6\times10^{14}$ cm^3s^{-1}*,” As you have done calculations, it would be better to state that the expts provide only an upper limit, and it is most likely that the *k* are smaller and closer to the theoretical values.

AUTHORS’ REPLY

Indeed, the actual value of k_{DMS+CI} would be smaller than the upper limits we reported, and the actual value of $k_{DMS+CH2OO}$ may be closer to the theoretical value ($k_{DMS+CH2OO}$ = 5.5×10^{-19} cm^3 s^{-1}). However, the calculation is not at the best level (while it is still good enough for the discussion in this paper) and there are uncertainties in the calculated values. Thus we decided not to say that the rate coefficients would be closer to the theoretical values.

Line 203 “*[CI]ss is expected to be low, at least a couple of orders of magnitude lower than the steady-state [OH]ss.*” On this basis, reactions need to be two orders of magnitude faster than OH to compete. SO2, H2O vapour and acids fit the bill but not many other reagents.

AUTHORS’ REPLY

We totally agree with your point. Thus we think the reaction of CI+DMS would not be a major path for the oxidization of DMS since the rate coefficient of CI+DMS is quite small.

Line 216 *“While our direct measurements and kinetics are very straightforward, the ozonolysis experiments of Newland et al. might have been more complex than the authors (Newland et al., 2015) had assumed. For example, one may consider the possibility of converting DMS to SO2 via surface or gas-phase reactions (Chen et al., 2018) under the complicated conditions of isoprene ozonolysis.*”

Is this a reasonable conclusion? In the introduction, you mentioned that prior to direct time-

resolved experiments, Criegee + SO_2 rate coefficients were thought to be slow. Is this another example of "surface" reactions? Is there more going in these ozonolysis experiments that bring about chemical change that if not captured by these direct measurements. Or are these relative rate reactions simply flawed?

Are there any suggested DMS → SO_2 schemes via the gas-phase?

AUTHORS' REPLY

The reviewer raised a few important and interesting questions, which are awaiting more investigations. As mentioned before, researchers have to postulate the reaction mechanism of the ozonolysis reaction to deduce the rate coefficients. We believe there are more to be studied for the ozonolysis of isoprene. For clarification, we would modify the related text to the following.

"For the determination of the relative rate of the CI + DMS reaction, Newland et al. monitored the consumption of SO_2 over a measurement period of up to 60 min until approximately 25% of isoprene was consumed (Newland et al., 2015). Additional uncharacterized reaction pathways (e.g., reactions with the products) would lead to a bias in the inferred rate coefficients. A part of this high complexity of the isoprene-ozone-DMS-SO_2 system has been discussed by Newland et al. in the section of Experimental Uncertainties (Newland et al., 2015). Our direct measurements and kinetics are very straightforward; the obtained results for individual CIs may provide useful constraints for related ozonolysis systems."

Line 220 Any reason why MKVOO + SO_2 not calculated?

AUTHORS' REPLY

We guess the reviewer meant MVKO+DMS. Now we have the calculation result of MVKO+DMS reaction. Similar to the reaction with H_2O (Vereecken et al., 2017), the direct reaction of *E*- and *Z*-MVKO with DMS is expected to be slower than for CH_2OO, as the organic groups and the conjugation of the carbonyl oxide moiety with the double bond stabilizes the CI. Indeed, for MVKO (all conformers), no adduct seems to exist at the M06-2X/cc-pVDZ level of theory: the needed C−S bond in the adduct appears to be too weak to

compensate for the loss of the conjugation in the carbonyl oxide, and the system reverts to the MVKO + DMS complex instead, without a formal C−S bond. As a result, the barrier for the migration of a DMS methyl H-atom to the carbonyl oxide oxygen to form a methylidene adduct is ~10 kcal/mol higher than for the analogous TS in the CH_2OO+DMS system which does feature a weakly bonded intermediate adduct. The direct oxygen transfer from *E*- or *Z*-MVKO to DMS, forming MVK + DMSO, was found to have a similarly high energy barrier as in the CH_2OO+DMS system. No viable reaction channels were found involving the double bond in MVKO. The lack of accessible transition states then prohibits rapid direct reaction between DMS and MVKO.

We also have additional calculation on the cyclisation of MVKO in the presence of DMS. Again, no accessible pathways were found.

TYPOS / UNDERSTANDING

Is it MKVO or MVKOO? I think the later. This occurs several times

Also, MACRO or MACROO?

AUTHORS' REPLY

MVKO is short for methyl-vinyl-ketone-oxide, and is the correct notation (i.e. MVK + 1 oxide O-atom). Likewise, MACRO is an acronym for methacroleine-oxide. We have standardized on these notations, consistent with our previous paper (Lin et al., 2020).

Line 74 "ozonlolysis" Typo

AUTHORS' REPLY

(will be fixed). Thanks for your reminder.

Line 91 "However, DMS absorbs weakly at 248 nm. We therefore performed additional experiments by photolyzing CH2I2 at 248 nm to assess the impact of DMS photolysis at 248 nm on the decay of the CIs."

Do you mean 308 nm?

AUTHORS' REPLY

We want to emphasize that DMS absorbs weakly at 248 nm ($\sigma = 1.28\times10^{-20}$ cm^2) but barely absorbs at 308 nm ($\sigma < 1\times10^{-22}$ cm^2) (Limão-Vieira et al., 2002). At low [DMS], the weak absorption of DMS at 248 nm may not cause a problem, but in this work, [DMS] is quite high and thus the photolysis of DMS at 248 nm should be taken into consideration.

Line 63 "*Newland et al. noted, however, that the presented rate coefficients do not correspond to the rates of single elementary reactions but rather describe the general reactivity of CIs towards DMS or H2O*" Can you re-phrase this as I'm not sure the point you making, be more explicit.

AUTHORS' REPLY:

Thank you for pointing out. The sentences will be rephrased to

"*Newland et al., who used ozonolysis of isoprene to generate a mixture of CIs (CH_2OO, MVKO, and MACRO), reported a combined reactivity of these CIs toward DMS and H_2O under conditions similar to the atmospheric boundary layer. Their reported rate coefficients might not correspond to those of single elementary reactions.*"

Line 36 Beames et al., 2013 This is a depletion experiment.

AUTHORS' REPLY:

Thank you for pointing out. The sentence will be rephrased to

"*… UV-visible absorption/depletion spectroscopy …*"

Anonymous referee 2:

One reason for the difference is the current results and the results reported in Newland 2015 may be the impact of DMS on the MVKO + SO_2 reaction. It is not necessary to perform calculations on this reaction, but some mechanistic discussion would be pertinent.

AUTHORS' REPLY:

The reactions of carbonyl oxides (CI) with SO_2 proceed by a barrierless cycloaddition (Kuwata et al., J. Phys. Chem. A, 119, 10316, 2015) with a very fast capture rate coefficient for complex formation near the collision limit, and a partial redissociation to the free reactants leading to a rate coefficient somewhat below the collision limit. The DMS-complex of a CI reacting with SO_2 can be expected to have a lower rate coefficient than the direct CI+SO_2 reaction, as the DMS shields part of the approach vectors of the SO_2 reactant, and the long-range attractive force is diminished due to a somewhat lower dipole moment of the complex compared to the free CI. However, the reduction of the rate coefficient is not expected to be all that large, and more importantly the CI+DMS complex is not overly strong such that only a small fraction of the CI will be present as a CI+DMS complex. This makes it hard to understand how DMS could affect any CI+SO_2 capture reaction (CH_2OO, MVKO, or CH_3CHOO) to the extent observed in Newland et al. It is for this reason that we have done exploratory calculations on the redissociation of the CI+SO_2 cyclo-adduct, but have found no indication that this would have the required impact on the effective CI+DMS rate of product formation.

Line 224: What is the evidence for the CH_2OO-DMS adduct having "very strong zwitterionic character?"

AUTHORS' REPLY:

At the level of theory used here, the wavefunction for the adduct converges to a closed-shell structure with no biradical character, where the O-atoms have a strongly negative partial charge (up to -0.46 in the Mulliken population analysis), and where the S-atom is positively charged S-atom (+0.28 in the Mulliken population analysis, compared to the Mulliken partial charge of -0.06 in DMS). This suggests that the CH_2OO-DMS adduct, similar to the parent

carbonyl oxide, has a zwitterionic character with very strong charge separation between the S and O atoms, rather than a biradical wavefunction.

Supplemental Information S20-S21: The authors should present some calculations on the MVKO. In particular, it would be worthwhile to consider how DMS might affect the cyclization of the anti conformer of MVKO to the dioxole (see J. Am. Chem. Soc. 2018, 140, 10866). Here, I reiterate the comment of Rickard that it would be useful for the authors to estimate the relative amounts of the syn and anti conformers of MVKO.

AUTHORS' REPLY:

The dominant unimolecular reaction of *E*-MVKO is a 1,4-H-shift (VHP-channel), analogous to *Z*-CH_3CHOO, for which we already showed that any catalytic effect is insufficient to allow for fast reactions. We now also calculated the impact of a DMS spectator complexing agent on the cyclization in *Z*-MVKO at the M06-2X/cc-pVDZ level of theory, finding similar results as for the methylated CH_3CHOO, i.e. the barrier height without (12.1 kcal/mol) and with complexing DMS (14.2 kcal/mol from the ground state of the complex) are essentially identical. The complex stability for *Z*-MVKO + DMS (−9.9 kcal/mol) is also similar to that for CH_2OO, *Z*-CH_3CHOO, and *E*-CH_3CHOO. Any catalyzing effect by DMS would then be due to chemical activation by the energy released in the complexation. The net energy barrier for the DMS catalysed *Z*-MVKO unimolecular reaction is ~ +4 kcal/mol, then still implies a slow bimolecular reaction, in agreement with the experimental observations.

Also see Reply to Referee 1 (for Line 220) for the calculation results on the direct reaction of MVKO + DMS.

Regarding the relative amounts of the *syn* and *anti* conformers of MVKO, we would add the following sentences to clarify the MVKO conformation. (after line 80)

"*For MVKO, there are 4 possible conformers. Following the nomenclature of Barber et al., syn/anti-MVKO (E/Z-MVKO) has a methyl/vinyl group at the same side of the terminal oxygen, while cis and trans refer to the orientation between the vinyl C=C and the carbonyl C=O bonds (Barber et al., 2018). It has been reported that syn- and anti-MVKO do not interconvert due to a high barrier between them but the barrier between cis and trans forms is low enough to permit fast interconversion at 298 K (Barber et al., 2018;Vereecken et al., 2017). Caravan et al., have shown that anti-MVKO is unobservable under thermal (298 K) conditions due to short lifetime and/or low yield, and thus, the UV-Vis absorption signal is from an equilibrium mixture of cis and trans forms of syn-MVKO (Caravan et al., 2020;Vereecken et al., 2017). For simplicity we will use MVKO to represent syn-MVKO (E-MVKO).*"

Lines 232-233: "*We did not examine more exotic CI reaction such as insertion in the DMS C–H bonds, as these are known to have comparatively high barriers.*" This statement should have a reference.

AUTHORS' REPLY:

We would add the paper of (Decker et al. ***Phys. Chem. Chem. Phys.***, 2017,**19**, 8541-8551, doi:10.1039/C6CP08602K) into the reference

Supplemental Information S20-S21: The authors should tabulate the relative energies predicted by the M06-2X/cc-pVDZ calculations.

AUTHORS' REPLY:

A table is now included in the supporting information.

Table S_: ZPE-corrected DMS complex energies, E(complex), and barrier heights E_b without and with a DMS complexing agent, at the M06-2X/cc-pVDZ level of theory. Energies are in kcal mol^{-1} and relative to the free reactants.

CI reaction	E_b	E(complex)	E_b(complex)
$CH_2OO \rightarrow$ cyc-CH_2OO-	22.0	-9.6	14.5
Z-$CH_3CHOO \rightarrow CH_2CHOOH$	12.7	-8.6	7.2
Z-$CH_3CHOO \rightarrow$ cyc-$CH(CH_3)OO$-	25.8	-8.6	18.2
E-$CH_3CHOO \rightarrow$ cyc-$CH(CH_3)OO$-	18.4	-10.9	9.5
Z-$(CH{=}CH_2)C(CH_3)OO \rightarrow$ cyc-CH-$CH_2C(CH_3)OO$-	12.1	-9.9	4.4
Z-$(CH{=}CH_2)C(CH_3)OO$ + DMS → MVK + DMSO	8.7		
E-$(CH_3)C(CH{=}CH_2)OO$ + DMS → MVK + DMSO	8.0		
$(CH_3)C(CH{=}CH_2)OO$ + DMS → $S(CH_3)(=CH_2)C(CH_3)(CH{=}CH_2)OOH$	11.2		

Anonymous Referee #3

Received and published: 30 July 2020

Kuo et al. report direct experimental and theoretical investigations of the reactions of two isoprene-derived Criegee intermediates with dimethyl sulfide (DMS). Using the diiodoalkane/diiodoalkene photolysis method to selectively generate each Criegee intermediate in turn, the authors probe the kinetics by UV absorption and deduce upper limit rate coefficients that are orders of magnitude slower than those obtained in the ozonolysis work of Newland et al. using the relative rate technique. The slow rate coefficient measured in the present work for CH2OO + DMS is substantiated by stationary point calculations coupled with CTST that yield a rate coefficient of 5.5E-19 cm-3 s-1 at 298 K.

The paper is reasonably thorough and raises interesting discussion about ozonolysis vs. direct Criegee intermediate experimental kinetic studies, that have been significantly expanded by the other reviewers. The paper would benefit from some points of clarification (suggested below) and additional theoretical work on the MVK-oxide + DMS reaction to compare with the experimental results and contrast with the calculations on the CH2OO system. Please note that many of the comments in this review reflect the points that have already been raised in the thorough reviews of Rickard. Newland and Bloss, Blitz and the anonymous reviewer.

Main text

Page 2, line 33: The Welz et al. 2012 work is preceded by the Taatjes et al. JACS paper in which DMSO was used to generate the CH2OO Criegee intermediate.

AUTHORS' REPLY:

The reviewer is correct. However, the method reported by Taatjes et al.(Taatjes et al., 2008) is less efficient than that by Welz et al. (Welz et al., 2012) Nowadays, most photolytic generation of Criegee intermediates follow the method by Welz et al. The related sentences

"However, due to their high reactivity and, hence, short lifetimes, laboratory studies of the reactions of CIs have been challenging. In fact, no direct detection of CIs has been known before Welz et al. reported a novel method to efficiently generate CIs other than through ozonolysis of alkenes (Welz et al., 2012)."

would be modified to

"However, due to their high reactivity and, hence, short lifetimes, laboratory studies of the reactions of CIs have been challenging until the work by Welz et al. who reported a novel

method to efficiently generate CIs other than through ozonolysis of alkenes (Welz et al., 2012).”

Page 2, line 41: It is already established that ozonolysis experiments are by their very nature complicated – the authors should instead be more specific about the potential concerns they have regarding obtaining rate coefficients of Criegee intermediates from ozonolysis studies.

AUTHORS’ REPLY:

We will clarify the situation by revising the related text to

“Surprisingly, the obtained rate coefficients are up to 10^4 times larger than previous results deduced from ozonolysis experiments (Johnson and Marston, 2008; Johnson et al., 2001; Hatakeyama and Akimoto, 1994). For ozonolysis experiments, typically only the ratios of reaction rate coefficients are obtained. The researchers have to compare with (at least) one absolute rate coefficient to get the rest rate coefficients. Unfortunately, the selected absolute rate coefficient (at that time) has large uncertainty, which propagates to other reported values. In addition, the reaction mechanism may be rather complicated and even the ratios of the rate coefficients need to be treated with care.”

Page 2, line 51: The very recent Cox et al. paper in ACPD (https://www.atmos-chemphys-discuss.net/acp-2020-472/) is also a thorough and up-to-date reference for existing studies of Criegee intermediate kinetics.

AUTHORS’ REPLY:

Thanks. We will include this new reference. (Cox et al., 2020)

Page 3, line 90: A reference (or some further explanation) is needed regarding the MVKO precursor absorption at 308 nm.

AUTHORS’ REPLY:

Below would be the measured absorbance of the diiodomethane (Exp# 12) and 1,3-diiodo-2-butene (Exp# 15) in the absorption cell (they are much diluted in the reactor cell). The absorption of 1,3-diiodo-2-butene at 308 nm is c.a. one-tenth of that at 248 nm. Consequently, we only perform the photolysis of 1,3-diiodo-2-butene at 248 nm.

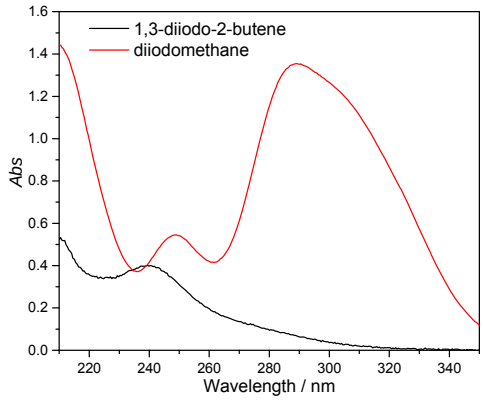

Page 4, line 110: The authors should be able to determine an approximation of at least the MVK-oxide precursor concentration in their system. The vapor pressure of the precursor can be estimated using the Antoine coefficients. If the precursor was delivered to the reactor via a bubbler at a known flow rate, then the approximate concentration of the precursor can be deduced. In the event that the absorption coefficient of the precursor is deduced at a later date, this information would enable the concentration of MVK-oxide used in the present work to be obtained.

AUTHORS' REPLY:

Currently we don't have the available data for the cross section nor the empirical coefficients of Antoine coefficients for 1,3-diiodo-2-butene; hence we couldn't derive the absolute concentration. We have reported the deduced absorbance (*Abs*) of the precursor in the photolysis cell of different experiments sets in Table S3. The absolute concentration of precursor can be deduced from the *Abs* of precursor and other experimental conditions shown in Table S3., once the absolute cross section of 1,3-diiodo-2-butene is available.

We have modified the text to

"However, because no absolute absorption cross sections for 1,3-diiodo-2-butene have been reported, its absolute concentration cannot be determined. We alternatively report the absorbance (Precursor Abs) of 1,3-diiodo-2-butene in the photolysis reactor (Table S3)."

Page 6, line 159: Under the present experimental conditions, CH_3 would most likely undergo reaction with O_2 to form CH_3OO and so it would be best to compare the reactivity of CH_3OO (rather than CH_3) with I atom and Criegee intermediates.

AUTHORS' REPLY:

Thanks for pointing out. We will revise the sentences to

"The expected products of DMS photolysis are CH_3 + CH_3S (Bain et al., 2018). Under the presence of O_2 (10 Torr), CH_3 would be converted into CH_3OO. These radicals (CH_3, CH_3OO, and CH_3S) are less reactive than I atoms or CIs."

Page 7, line 205: As the authors point out, there is currently significant uncertainty in the estimated and modelled steady state concentrations of Criegee intermediates. Because of this, it would be instructive to also frame the competitiveness of Criegee-initiated DMS oxidation vs. OH or NO3-initiated oxidation in terms of what concentration of Criegee intermediates are needed to oxidize a certain fraction (e.g. 5%, 10% or 20%) of atmospheric DMS using the theoretically determined rate coefficient.

AUTHORS' REPLY:

Possible concentrations of NO_3 and OH in the troposphere are found to be:

[OH] = 1×10^6 cm^{-3} (Li et al., 2018) and [NO_3] = 10 ppt = 2.5×10^8 cm^{-3} (Khan et al., 2015). Together with the reaction rate coefficients (k_{DMS+OH} = 4.8×10^{-12} cm^3 s^{-1}, $k_{DMS+NO3}$ = 6.8×10^{-11} cm^3 s^{-1} (Atkinson et al., 2004)), the concentration of CIs would have to be unreasonably high, at the order of 10^{11} cm^{-3}, to be competitive (5% of the effective reaction rate) with the DMS+OH and DMS+NO_3 reactions.

We would add the following sentences

"If the DMS reactions with CIs were to be competitive to those with NO_3 (e.g., 2.5×10^8 cm^{-3}) and OH (e.g., 1×10^6 cm^{-3}) (e.g., 5% of the overall DMS removal), the concentration of CIs would have to be unreasonably high, at the order of 10^{11} cm^{-3}."

Page 8, line 220. It seems peculiar that you have chosen to investigate theoretically only the CH2OO reaction and not the MVK-oxide reaction also. In MVK-oxide, the conjugation of the unsaturated side chain with the carbonyl oxide group has the potential to substantially

alter the surface. These calculations are likely significantly more complex than for the CH2OO case because of the need to consider syn and anti conformers, and cis/trans forms of each of these. However, given the interesting structural and conformeric dependence of Criegee intermediate reactivity, it is a regretful omission.

AUTHORS' REPLY:

Now we have the calculation result of MVKO+DMS reaction. Please see Reply to Referee 1 (for Line 220) for the calculation results on the direct reaction of MVKO + DMS, and the reply to referee 2 for catalysis reactions by DMS on unimolecular reactions of MVKO.

Page 8, line 233: A reference is needed to substantiate the statement regarding high barriers for DMS C-H insertion.

AUTHORS' REPLY:

We would add the paper of Decker et al. (***Phys. Chem. Chem. Phys.***, 2017,**19**, 8541-8551, doi:10.1039/C6CP08602K) in to the reference

Page 8, line 251: Do you anticipate stabilization of the (CH3)2SCH2OO adduct under tropospheric conditions?

The bonding is too weak to be stabilized under tropospheric conditions.

Page 9, line 261: You hypothesize that surface reactions converting DMS to SO2 in the chamber study of Newland could be the source of discrepancy between the present work and the work of Newland et al. I encourage the authors to respond to the comments of Rickard, Newland and Bloss, and Blitz regarding this matter.

AUTHORS' REPLY:

We would respond to the comments of Rickard et al. separately in the online discussion system of ACP.

Figure 2: Please include a note to address if the error bars are included or not included on this plot (as noted for Figure 4). Given that the rate coefficients for the self-reaction of CH2OO and the reaction of CH2OO + I (see Blitz review) are now well established, it would

be pertinent to deduce which of these is the major source of increased loss rates at higher laser fluence are under your experimental conditions.

AUTHORS' REPLY:

(i) We would add the following text in the caption:

"For each data point, the error of the single exponential fitting is less than 1% (thus not shown)."

(ii) Based on the absolute absorption cross section of CH_2OO at 340 nm ($\sigma = 1.23\times10^{-17}$ cm^2) and the pressure-dependent yield of CH_2OO from $CH_2I + O_2$ (0.46 at 300 Torr) (Ting et al., 2014a) the number densities of relevant species can be estimated to be the following (for Exp#1, Table S1).

$[CH_2OO]_0 = 6.7\times10^{11}$ cm^{-3}; $[I]_0 = 2.1\times10^{12}$ cm^{-3}; $[CH_2IOO]_0 = 7.7\times10^{11}$ cm^{-3}.

The first-order decay rate coefficient of CH_2OO (k_{eff}) can be approximately estimated (Li et al., 2020) as:

$$k_{eff} = k_I[I]_0 + k_{self}[CH_2OO]_0$$

Using $k_{self} = 8\times10^{-11}$ cm^3 s^{-1} and $k_I = 5.8\times10^{-11}$ cm^3 s^{-1} at 300 Torr (Mir et al., 2020), the estimated k_{eff} is 180 s^{-1}, consistent with the observed value of 232 s^{-1} for k_0. Therefore, the main loss processes of CH_2OO are reaction with iodine atoms (and other radicals) and its self-reaction.

In Figure S7, we can see a nice linear relationship between k_0 and the total produced radicals (proportional to the product of the laser fluence and the precursor concentration), further supporting the above mechanism. We would add the following sentences in the caption of Figure S7.

"The main loss processes of CH_2OO are reactions with radical byproducts like iodine atoms and its self-reaction. The observed values of k_0 (e.g., 232 s^{-1} for Exp#1) are consistent with the values (e.g., 180 s^{-1} at the condition of Exp#1) that are estimated using the reported kinetic data (yield and rate coefficients) (Mir et al., 2020; Ting et al., 2014)."

Supplementary information

Table S3: Because both the reaction forming MVK-oxide from the precursor + O2 reaction

as well as the MVK-oxide + SO2 reaction features an adduct, the authors should label more caerefully the adduct referred to in the 'adduct yield' column of the table to avoid confusion.

AUTHORS' REPLY: We will add a footnote after the "adduct yield[a]"

[a] *The yield of $CH_3(C_2H_3)ClOO$.*

Figures S1, S2: Provide details about error bars (c.f. comment about Figure 2).

AUTHORS' REPLY:

We would add the following text into the caption

"For each data point, the error of the single exponential fitting is lees than 1% (thus not shown)."

Figure S4: Please discuss the proposed origin of the "spike" at time zero.

AUTHORS' REPLY:

The photolysis of DMS produces radicals like CH_3 and CH_3S. A few vibronic bands of the A-X transition of the CH_3S radical (Liu et al., 2005) are within our probe window (335-345 nm). Thus it is possible that the "spike" near time zero is due to the absorption of the radical products of DMS photolysis, likely CH_3S or vibrationally excited CH_3S. We would add the following sentence in the figure caption.

"The absorbance change under zero [DMS] comes from the interaction of the optics and the photolysis laser pulse, whereas the "spike" near time zero at high [DMS] may come from the absorption of the radical products of DMS photolysis, likely CH_3S (Liu et al., 2005) and/or vibrationally excited CH_3S."

S10: These additional investigations are illuminating and interesting.

AUTHORS' REPLY: Thanks.

Additional comments regarding MVK-oxide conformers

I would like to add some discussion to the comments made by other reviewers regarding which conformers of MVK-oxide are produced from the photolytic scheme vs. ozonolysis. While the distribution of these conformers has not yet been deduced, the recent literature on

direct MVK-oxide kinetic and spectroscopic studies that indicated that both syn (Caravan et al., 2020) and anti (Vansco et al., 2020) confirmers are produced from the 1,3,-diiodobut-2-ene photolysis scheme used in the present work (Barber et al., 2018). Additionally, due to the rapid unimolecular decay of anti compared with syn (Barber et al., 2018;Vereecken et al., 2017), it is unlikely that reaction with DMS could compete with unimolecular decay under tropospheric conditions for the anti conformer.

AUTHORS' REPLY:

Same as the reply to Referee 2 (for Supplemental Information S20-S21), we have added some description to after line 80 to clarify the MVKO conformation.

"*For MVKO, there are 4 possible conformers. Following the nomenclature of Barber et al., syn/anti-MVKO (E/Z-MVKO) has a methyl/vinyl group at the same side of the terminal oxygen, while cis and trans refer to the orientation between the vinyl C=C and the carbonyl C=O bonds (Barber et al., 2018). It has been reported that syn- and anti-MVKO do not interconvert due to a high barrier between them but the barrier between cis and trans forms is low enough to permit fast interconversion at 298 K (Barber et al., 2018;Vereecken et al., 2017). Caravan et al., have shown that anti-MVKO is unobservable under thermal (298 K) conditions due to short lifetime and/or low yield, and thus, the UV-Vis absorption signal is from an equilibrium mixture of cis and trans forms of syn-MVKO (Caravan et al., 2020;Vereecken et al., 2017). For simplicity we will use MVKO to represent syn-MVKO (E-MVKO).*"

References:

Atkinson, R., Baulch, D. L., Cox, R. A., Crowley, J. N., Hampson, R. F., Hynes, R. G., Jenkin, M. E., Rossi, M. J., and Troe, J.: Evaluated kinetic and photochemical data for atmospheric chemistry: Volume I - gas phase reactions of O_x, HO_x, NO_x and SO_x species, Atmos. Chem. Phys., 4, 1461-1738, https://doi.org/10.5194/acp-4-1461-2004, 2004.

Bain, M., Hansen, C. S., and Ashfold, M. N. R.: Communication: Multi-mass velocity map imaging study of the ultraviolet photodissociation of dimethyl sulfide using single photon ionization and a PImMS2 sensor, J. Chem. Phys., 149, 081103, 10.1063/1.5048838, 2018.

Barber, V. P., Pandit, S., Green, A. M., Trongsiriwat, N., Walsh, P. J., Klippenstein, S. J., and Lester, M. I.: Four-Carbon Criegee Intermediate from Isoprene Ozonolysis: Methyl Vinyl Ketone Oxide Synthesis, Infrared Spectrum, and OH Production, J. Am. Chem. Soc., 140, 10866-10880, 10.1021/jacs.8b06010, 2018.

Caravan, R. L., Vansco, M. F., Au, K., Khan, M. A. H., Li, Y.-L., Winiberg, F. A. F., Zuraski, K., Lin, Y.-H., Chao, W., Trongsiriwat, N., Walsh, P. J., Osborn, D. L., Percival, C. J., Lin, J. J.-M., Shallcross, D. E., Sheps, L., Klippenstein, S. J., Taatjes, C. A., and Lester, M. I.: Direct kinetic measurements and theoretical predictions of an isoprene-derived Criegee intermediate, Proc. Natl. Acad. Sci., 117, 9733-9740, 10.1073/pnas.1916711117, 2020.

Cox, R. A., Ammann, M., Crowley, J. N., Herrmann, H., Jenkin, M. E., McNeill, V. F., Mellouki, A., Troe, J., and Wallington, T. J.: Evaluated kinetic and photochemical data for atmospheric chemistry: Volume VII - Criegee intermediates, Atmos. Chem. Phys. Discuss., 2020, 1-41, 10.5194/acp-2020-472, 2020.

Decker, Z. C. J., Au, K., Vereecken, L., and Sheps, L.: Direct experimental probing and theoretical analysis of the reaction between the simplest Criegee intermediate CH_2OO and isoprene, Phys. Chem. Chem. Phys., 19, 8541-8551, 10.1039/C6CP08602K, 2017.

Hatakeyama, S., and Akimoto, H.: Reactions of criegee intermediates in the gas phase, Res. Chem. Intermed., 20, 503-524, 10.1163/156856794X00432, 1994.

Johnson, D., Lewin, A. G., and Marston, G.: The Effect of Criegee-Intermediate Scavengers on the OH Yield from the Reaction of Ozone with 2-methylbut-2-ene, J. Phys. Chem. A, 105, 2933-2935, 10.1021/jp003975e, 2001.

Johnson, D., and Marston, G.: The gas-phase ozonolysis of unsaturated volatile organic compounds in the troposphere, Chem. Soc. Rev., 37, 699-716, 10.1039/B704260B, 2008.

Khan, M. A. H., Cooke, M. C., Utembe, S. R., Archibald, A. T., Derwent, R. G., Xiao, P., Percival, C. J., Jenkin, M. E., Morris, W. C., and Shallcross, D. E.: Global modeling of the nitrate radical (NO_3) for present and pre-industrial scenarios, Atmospheric Research, 164-165, 347-357, https://doi.org/10.1016/j.atmosres.2015.06.006, 2015.

Kuwata, K. T., Guinn, E. J., Hermes, M. R., Fernandez, J. A., Mathison, J. M., and Huang, K.: A Computational Re-examination of the Criegee Intermediate–Sulfur Dioxide Reaction, J. Phys. Chem. A, 119, 10316-10335, 10.1021/acs.jpca.5b06565, 2015.

Li, M., Karu, E., Brenninkmeijer, C., Fischer, H., Lelieveld, J., and Williams, J.: Tropospheric OH and stratospheric OH and Cl concentrations determined from CH_4, CH_3Cl, and SF_6 measurements, npj Climate and Atmospheric Science, 1, 29, 10.1038/s41612-018-0041-9, 2018.

Li, Y.-L., Kuo, M.-T., and Lin, J. J.-M.: Unimolecular decomposition rates of a methyl-substituted Criegee intermediate *syn*-CH_3CHOO, RSC Advances, 10, 8518-8524, 10.1039/D0RA01406K, 2020.

Limão-Vieira, P., Eden, S., Kendall, P. A., Mason, N. J., and Hoffmann, S. V.: High resolution VUV photo-absorption cross-section for dimethylsulphide, $(CH_3)_2S$, Chemical Physics Letters, 366, 343-349, https://doi.org/10.1016/S0009-2614(02)01651-2, 2002.

Lin, Y.-H., Li, Y.-L., Chao, W., Takahashi, K., and Lin, J. J.-M.: The role of the iodine-atom adduct in the synthesis and kinetics of methyl vinyl ketone oxide—a resonance-stabilized Criegee intermediate, Phys. Chem. Chem. Phys., 22, 13603-13612, 10.1039/D0CP02085K, 2020.

Liu, C.-P., Reid, S. A., and Lee, Y.-P.: Two-color resonant four-wave mixing spectroscopy of highly predissociated levels in the $\tilde{A}A_{12}$ state of CH_3S, J. Chem. Phys., 122, 124313, 10.1063/1.1867333, 2005.

Mir, Z. S., Lewis, T. R., Onel, L., Blitz, M. A., Seakins, P. W., and Stone, D.: CH_2OO Criegee intermediate UV absorption cross-sections and kinetics of CH_2OO + CH_2OO and CH_2OO + I as a function of pressure, Phys. Chem. Chem. Phys., 22, 9448-9459, 10.1039/D0CP00988A, 2020.

Newland, M. J., Rickard, A. R., Vereecken, L., Muñoz, A., Ródenas, M., and Bloss, W. J.: Atmospheric isoprene ozonolysis: impacts of stabilised Criegee intermediate reactions with SO_2, H_2O and dimethyl sulfide, Atmos. Chem. Phys., 15, 9521-9536, 10.5194/acp-15-9521-2015, 2015.

Smith, M. C., Chao, W., Takahashi, K., Boering, K. A., and Lin, J. J. M.: Unimolecular Decomposition Rate of the Criegee Intermediate $(CH_3)_2COO$ Measured Directly with UV Absorption Spectroscopy, J. Phys. Chem. A, 120, 4789-4798, 10.1021/acs.jpca.5b12124, 2016.

Taatjes, C. A., Meloni, G., Selby, T. M., Trevitt, A. J., Osborn, D. L., Percival, C. J., and Shallcross, D. E.: Direct Observation of the Gas-Phase Criegee Intermediate (CH_2OO), J. Am. Chem. Soc., 130, 11883-11885, 10.1021/ja804165q, 2008.

Ting, W. L., Chang, C. H., Lee, Y. F., Matsui, H., Lee, Y. P., and Lin, J. J. M.: Detailed mechanism of the $CH_2I + O_2$ reaction: Yield and self-reaction of the simplest Criegee intermediate CH_2OO, J. Chem. Phys., 141, 104308, 10.1063/1.4894405, 2014a.

Ting, W. L., Chen, Y. H., Chao, W., Smith, M. C., and Lin, J. J. M.: The UV absorption spectrum of the simplest Criegee intermediate CH_2OO, Phys. Chem. Chem. Phys., 16, 10438-10443, 10.1039/c4cp00877d, 2014b.

Vansco, M. F., Caravan, R. L., Zuraski, K., Winiberg, F. A. F., Au, K., Trongsiriwat, N., Walsh, P. J., Osborn, D. L., Percival, C. J., Khan, M. A. H., Shallcross, D. E., Taatjes, C. A., and Lester, M. I.: Experimental Evidence of Dioxole Unimolecular Decay Pathway for Isoprene-Derived Criegee Intermediates, J. Phys. Chem. A, 124, 3542-3554, 10.1021/acs.jpca.0c02138, 2020.

Vereecken, L., Novelli, A., and Taraborrelli, D.: Unimolecular decay strongly limits the atmospheric impact of Criegee intermediates, Phys. Chem. Chem. Phys., 19, 31599-31612, 2017.

Welz, O., Savee, J. D., Osborn, D. L., Vasu, S. S., Percival, C. J., Shallcross, D. E., and Taatjes, C. A.: Direct Kinetic Measurements of Criegee Intermediate (CH_2OO) Formed by Reaction of CH_2I with O_2, Science, 335, 204-207, 10.1126/science.1213229, 2012.

Kinetics of dimethyl sulfide (DMS) reactions with isoprene-derived Criegee intermediates studied with direct UV absorption

Mei-Tsan Kuo[1], Isabelle Weber[2,6], Christa Fittschen[2], Luc Vereecken[3,4], Jim Jr-Min Lin[1,5]

[1]Institute of Atomic and Molecular Sciences, Academia Sinica, Taipei 10617, Taiwan
[2]Univ. Lille, CNRS, UMR 8522 - PC2A - Physicochimie des Processus de Combustion et de l'Atmosphère, F-59000 Lille, France
[3]Max Planck Institute for Chemistry, Hahn-Meitner-Weg 1, 55128 Mainz, Germany
[4]Institute for Energy and Climate Research, IEK-8: Troposphere, Forschungszentrum Jülich GmbH, 52428 Jülich, Germany
[5]Department of Chemistry, National Taiwan University, Taipei 10617, Taiwan
[6]Present address: Department of Applied Chemistry and Institute of Molecular Science, National Chiao Tung University, Hsinchu 30010, Taiwan

Correspondence to: Jim Jr-Min Lin (jimlin@gate.sinica.edu.tw)

Abstract. Criegee intermediates (CIs) are formed in the ozonolysis of unsaturated hydrocarbons and play a role in atmospheric chemistry as a non-photolytic OH source or a strong oxidant. Using a relative rate method in an ozonolysis experiment, Newland et al. [Atmos. Chem. Phys., 15, 9521-9536, 2015] reported high reactivity of isoprene-derived Criegee intermediates towards dimethyl sulfide (DMS) relative to that towards SO_2 with the ratio of the rate coefficients k_{DMS+CI} / k_{SO2+CI} = 3.5±1.8. Here we reinvestigated the kinetics of DMS reactions with two major Criegee intermediates formed in isoprene ozonolysis, CH_2OO and methyl vinyl ketone oxide (MVKO). The individual CI was prepared following reported photolytic method with suitable (diiodo) precursors in the presence of O_2. The concentration of CH_2OO or MVKO was monitored directly in real time through their intense UV-visible absorption. Our results indicate the reactions of DMS with CH_2OO and MVKO are both very slow; the upper limits of the rate coefficients are 4 orders of magnitude smaller than that reported by Newland et al. These results suggest that the ozonolysis experiment could be complicated such that interpretation should be careful and these CIs would not oxidize atmospheric DMS at any substantial level.

1 Introduction

As a non-photolytic OH source or a strong oxidant, Criegee intermediates (CIs) influence the chemical processes in the troposphere (Nguyen et al., 2016; Novelli et al., 2014; Johnson and Marston, 2008; Atkinson and Aschmann, 1993; Gutbrod et al., 1997; Zhang et al., 2002) and, ultimately, have impact on the formation of secondary aerosols and other pollutants (Percival et al., 2013; Wang et al., 2016; Meidan et al., 2019). A detailed understanding of CI chemistry under atmospheric conditions is, thus, necessary to be able to accurately predict and describe the evolution of Earth's atmosphere.

However, due to their high reactivity and, hence, short lifetimes, laboratory studies of the reactions of CIs have been challenging until the work by Welz et al. who reported a novel method to efficiently generate CIs other than through ozonolysis of alkenes (Welz et al., 2012). They utilized (R1) and (R2) to prepare CH_2OO and directly measured the rate coefficients of CH_2OO reactions with SO_2 and NO_2 by following the time-resolved decay of CH_2OO.

$$CH_2I_2 + h\nu \rightarrow CH_2I + I \quad \text{(R1)}$$

$$CH_2I + O_2 \rightarrow CH_2OO + I \quad \text{(R2)}$$

Surprisingly, the obtained rate coefficients are up to 10^4 times larger than previous results deduced from ozonolysis experiments (Johnson et al., 2001; Hatakeyama and Akimoto, 1994; Johnson and Marston, 2008). For ozonolysis experiments, typically only the ratios of certain reaction rate coefficients are obtained. The researchers have to compare with (at least) one absolute rate coefficient to get the rest rate coefficients. Unfortunately, the selected absolute rate coefficient (at that time) has large uncertainty, which propagates to other reported values. In addition, the reaction mechanism may be rather complicated and even the ratios of the rate coefficients need to be treated with care.

After this pioneering work, the same method has been applied for generation of other CIs, like CH_3CHOO (Taatjes et al., 2013), $(CH_3)_2COO$ (Liu et al., 2014a; Taatjes et al., 2013), methyl vinyl ketone oxide (MVKO) (Barber et al., 2018), methacrolein oxide (MACRO) (Vansco et al., 2019), etc. These CIs have been identified with various detection methods, like photoionization mass spectrometry (Taatjes et al., 2013), infrared action (Liu et al., 2014b) and absorption (Su et al., 2013; Lin et al., 2015) spectroscopy, UV-visible absorption/depletion spectroscopy (Liu et al., 2014a; Beames et al., 2013; Sheps, 2013; Smith et al., 2014; Chang et al., 2016; Ting et al., 2014), microwave spectroscopy (McCarthy et al., 2013; Nakajima et al., 2015), etc. In addition, utilizing the direct detection of CIs, a number of kinetic investigations of CI reactions, e.g., with SO_2 (Huang et al., 2015), water vapor (Chao et al., 2015), alcohols (Chao et al., 2019), thiols (Li et al., 2019), amines (Chhantyal-Pun et al., 2019), carbonyl molecules (Taatjes et al., 2012), and organic (Welz et al., 2014) and inorganic (Foreman et al., 2016) acids, etc., have been reported (Lee, 2015; Osborn and Taatjes, 2015; Lin and Chao, 2017; Khan et al., 2018; Cox et al., 2020).

Recently, Newland et al. studied the reactivity of CIs with H_2O and, for the first time, with dimethyl sulfide (DMS) in the ozonolysis of isoprene at the EUPHORE simulation chamber facility and found a rapid reaction of CIs with DMS (Newland et al., 2015). A mixture of CH_2OO, MVKO and MACRO was generated through ozonolysis of isoprene with a total CI yield of 0.56±0.03 (Newland et al., 2015). The relative yields of the individual CIs have previously been estimated to be 0.58/0.55 for CH_2OO, 0.23/0.37 for MVKO, and 0.19/0.08 for MACRO by an analysis based on a large laboratory, modelling and field data set (Nguyen et al., 2016) or an earlier theoretical calculation (Zhang et al., 2002). To determine reaction rates, Newland et al. used a relative rate method and followed the removal of SO_2 versus the removal of other reactants. For the reaction CI + DMS relative to the reaction CI + SO_2, they obtained a relative rate coefficient of $k_{DMS+CI} / k_{SO2+CI} = 3.5 \pm 1.8$ (Newland et al., 2015). Since the reactions of typical CIs with SO_2 are very fast, with rate coefficients on the order of 4×10^{-11} $cm^3\ s^{-1}$ (Welz et al., 2012; Lee, 2015; Osborn and Taatjes, 2015; Lin and Chao, 2017; Khan et al., 2018), this result

suggests that the reaction of CI + DMS is extremely fast, with a rate coefficient of ca. 10^{-10} cm^3 s^{-1}. This value is extremely large, close to those of the fastest reactions of CIs.

Newland et al., who used ozonolysis of isoprene to generate a mixture of CIs (CH_2OO, MVKO, and MACRO), reported a combined reactivity of these CIs toward DMS and H_2O under conditions similar to the atmospheric boundary layer (Newland et al., 2015). Their reported rate coefficients may not correspond to those of single elementary reactions.

DMS is the major sulfur containing species in the atmosphere with high abundances in the marine boundary layer (Yvon et al., 1996) but also e.g. in the Amazon basin (Jardine et al., 2015), and has been shown to play an important role in the formation of SO_2 and sulfuric acid, which are precursors of sulfide aerosols (Andreae and Crutzen, 1997; Charlson et al., 1987; Faloona, 2009). The results of Newland et al. (Newland et al., 2015) therefore suggest that in regions with high concentrations of CIs, the CI + DMS reactions will have a comparable impact on the oxidation of DMS, considering the main atmospheric oxidants are OH and NO_3 ($k_{DMS+OH} = 4.8\times10^{-12}$ cm^3 s^{-1}, $k_{DMS+NO3} = 1.1\times10^{-12}$ cm^3 s^{-1} (Atkinson et al., 2004)).

Here we report the first direct kinetic study of DMS reactions with CH_2OO and MVKO, the main CIs formed in the ozonolysis of isoprene. CIs have strong UV-visible absorption (Lin and Chao, 2017). For example, CH_2OO and MVKO absorb strongly (peak cross section $\sigma \geq 1\times10^{-17}$ cm^2) in the wavelength ranges of 285–400 nm (Ting et al., 2014; Lewis et al., 2015) and 315–425 nm (Vansco et al., 2018) (> 20% of the peak value), respectively. This strong and distinctive absorption has been utilized to probe CIs in a number of kinetic experiments, including their reactions with SO_2, water vapor, alcohols, thiols, organic and inorganic acids, carbonyl compounds, alkenes, etc. (Khan et al., 2018; Lin and Chao, 2017; Osborn and Taatjes, 2015; Lee, 2015). In this work, both CH_2OO and MVKO were directly probed in real time via their strong UV absorption at 340 nm. For MVKO, there are 4 possible conformers. Following the nomenclature of Barber et al., *syn*/*anti*-MVKO (*E*/*Z*-MVKO) has a methyl/vinyl group at the same side of the terminal oxygen, while *cis* and *trans* refer to the orientation between the vinyl C=C and the carbonyl C=O bonds (Barber et al., 2018). It has been reported that *syn*- and *anti*-MVKO do not interconvert due to a high barrier between them but the barrier between *cis* and *trans* forms is low enough to permit fast interconversion at 298 K (Barber et al., 2018; Vereecken et al., 2017). Caravan et al., have shown that *anti*-MVKO is unobservable under thermal (298 K) conditions due to short lifetime and/or low yield, and thus, the UV-Vis absorption signal is from an equilibrium mixture of *cis* and *trans* forms of *syn*-MVKO (Caravan et al., 2020; Vereecken et al., 2017). For simplicity we will use MVKO to represent *syn*-MVKO (*E*-MVKO).

Surprisingly, our experimental results do not indicate any significant reactivity of DMS with CH_2OO or MVKO. We therefore propose upper limits of the rate coefficients for these reactions. Implications for atmospheric chemistry are discussed.

2. Method

2.1 Experimental setup

The experimental setup has been described previously (Chao et al., 2019; Chao et al., 2015). To generate CH_2OO and MVKO, we followed the approaches of Welz et al. (Welz et al., 2012) and Barber et al., respectively. The MVKO formation is through the reaction sequence $ICH_2–CH=C(I)–CH_3 + h\nu \rightarrow CH_3(C_2H_3)CI + I$, $CH_3(C_2H_3)CI + O_2 \rightarrow MVKO + I$, analogue to reactions (R1) and (R2) (Barber et al., 2018). We applied a 308 nm photolysis laser (XeCl excimer laser) for generating CH_2OO, while a photolysis laser at 248 nm (KrF excimer laser) was used for generating MVKO because the MVKO precursor absorbs 308 nm photon too weakly. However, a small amount of DMS would absorb 248 nm light and dissociate; the photodissociated DMS may affect the kinetics of the CIs. We therefore performed additional experiments by photolyzing CH_2I_2 at 248 nm to assess the impact of DMS photolysis at 248 nm on the decay of the CIs.

Experiments were conducted in a photolysis reactor (inner diameter: 1.9 cm, effective length: 71 cm). The photolysis laser beam was coupled into and out of the reactor by two long-pass filters (248 nm: Eksma Optics, custom-made 275 nm long-pass; 308 nm: Semrock LP03-325RE-25) and monitored with an energy meter (Gentec EO, QE25SP-H-MB-D0). The probe light was from a plasma Xe lamp (Energetiq, EQ-99) (Su and Lin, 2013) and directed through the reactor collinearly with the photolysis beam. It passes through the reactor six times, resulting in an effective absorption path length of ca. 426 cm. After passing through band-pass filters (340 nm, Edmund, #65129, 10 nm bandwidth, OD 4), the probe beam and a reference beam which did not pass through the reactor were both focused on a balanced photodiode detector (Thorlabs, PDB450A). Output signals were recorded in real time with a high-resolution oscilloscope (LeCroy, HDO4034, 4096 vertical resolution) and averaged for 120 laser shots (repetition rate ~1 Hz). We observed a small time-dependent variation in transmittance even when no precursor was introduced into the reactor. To compensate for this effect, which was caused by the optics and the photolysis laser pulse, we recorded background traces without adding the precursor before and after each set of experiments. The reported data are after background subtraction.

All reactant gas flows were controlled by calibrated mass-flow controllers (Brooks: 5850E, 5800E and Bronkhorst: EL-FLOW prestige) and mixed before entering the reactor. Reactant concentrations were determined prior to the mixing of the reactant flows by UV absorption spectroscopy in two separate absorption cells for either DMS (absorption path length 90.4 cm for $[DMS] \leq 1.7\times10^{15}$ cm^{-3} or 20.1 cm for $[DMS] \leq 8.1\times10^{15}$ cm^{-3}) or the respective diiodo precursors (absorption path length 90.4 cm) using the reported absorption cross sections (Sander et al., 2011; Limão-Vieira et al., 2002). However, because no absorption cross sections for 1,3-diiodo-2-butene have been reported, its absolute concentration cannot be determined. We, thus, can only report the absorbance (Precursor *Abs*) of 1,3-diiodo-2-butene in the photolysis reactor (Table S3). Typical concentration ranges were: $[CH_2I_2]=(0.23–2.54)\times10^{14}$ cm^{-3}, $[O_2]=(3.28–3.30)\times10^{17}$ cm^{-3}, and $[DMS]=(0–8.1)\times10^{15}$ cm^{-3}. We assume ideal gas behavior for the concentration calculation. The majority of the experiments were performed at 300 Torr (N_2) and 298 K.

2.2 Theoretical methodology

The potential energy surface (PES) of the CH_2OO + DMS reaction was first explored at the M06-2X/cc-pVDZ level of theory (Dunning, 1989; Zhao and Truhlar, 2008), characterizing the geometries and rovibrational characteristics of the reactants, intermediates and transition states for a wide range of potential reaction channels. The pathways found were re-optimized with a larger basis set using M06-2X/aug-cc-pV(T+d)Z, where the triple-zeta basis set is enhanced by tight d-orbitals to improve the description of the sulfur atom bonds (Bell and Wilson, 2004; Dunning et al., 2001). Finally, CCSD(T)/aug-cc-pVTZ single point energy calculations were performed to obtain more reliable energies (Dunning, 1989; Purvis and Bartlett, 1982). The T_1 diagnostics, all ≤ 0.026 except for CH_2OO (0.042), suggest that the calculations are not affected by strong multi-reference character in intermediates or transition states. The molecular characteristics thus obtained were used in canonical transition state theory (CTST) calculations to derive the temperature-dependent rate coefficient $k(T)$ (Truhlar et al., 1996). All calculations were performed using the Gaussian-09 software suite (Frisch et al., 2009). The Supplement information discusses additional calculations.

3 Results and discussion

3.1. CH_2OO + DMS

Representative time traces of CH_2OO absorption recorded at 340±5 nm ($\sigma = 1.23\times10^{-17}$ cm^2 at 340 nm) (Ting et al., 2014) under various [DMS] are depicted in Fig. 1. Similar results but recorded with different initial concentrations of CH_2I_2 and/or different photolysis laser fluences are displayed in Figs. S12–S14. At $t = 0$, CH_2OO is generated within 10^{-5} s by photolysis of CH_2I_2 at 308 nm (nanosecond pulsed laser) (R1) and the fast reaction of CH_2I with O_2 (R2) ($k_{O2} = 1.4\times10^{-12}$ cm^3 s^{-1} (Eskola et al., 2006); $[O_2] = 3.3 \times 10^{17}$ cm^{-3}). The subsequent decay in absorption is due to the consumption of CH_2OO either through reaction with DMS or through other processes, e.g., bimolecular reactions with radical byproducts like I atoms, wall loss, etc. In addition, self-reaction of CH_2OO has been found to be rather fast ($k_{self} = 8\times10^{-11}$ cm^3 s^{-1}) (Mir et al., 2020). However, the effect of the self-reaction (Smith et al., 2016; Li et al., 2020) would not affect the determination of k_{DMS} under our experimental conditions. We can see that the decay curves of CH_2OO at various [DMS] are extremely similar to one another, indicating that the reaction of CH_2OO + DMS is not significant.

The decay of CH_2OO can be well described with an exponential function ($R^2 > 0.995$) (e.g., Fig. 1).

$$[CH_2OO](t) = [CH_2OO]_0 e^{-k_{obs}t} \quad (1)$$

The fitting error of k_{obs} is less than 1% mostly. Under the conditions of this study, the consumption of CH_2OO can be described as

$$-\frac{d[CH_2OO]}{dt} = k_{obs}[CH_2OO] = (k_0 + k_{DMS+CH2OO}[DMS])[CH_2OO] \quad (2)$$

where k_0 represents the sum of the effective rate coefficients for all consumption channels of CH_2OO except its reaction with DMS, which is described as the bimolecular rate coefficient $k_{DMS+CH2OO}$.

The CH_2OO decay rate coefficients k_{obs} as functions of [DMS] for different photolysis laser fluences are summarized in Fig. 2. At higher laser fluences, more CH_2OO and radical byproducts are generated, resulting in shorter CH_2OO lifetimes (see Fig. S7: plot of k_0 against $[CH_2I_2]\times I_{308nm}$), similar to previous works (Smith et al., 2016; Li et al., 2020; Zhou et al., 2019). The slopes of the linear fits of Fig. 2 would correspond to $k_{DMS+CH2OO}$ (see Eq. (2)). However, the slope values are quite small, close to our detection limit (Lin et al., 2018). Within experimental uncertainty, $k_{DMS+CH2OO}$ exhibits no clear correlation to the photolysis laser fluence and other experimental conditions like $[CH_2I_2]$ (see Table S1 and Fig. S9). From a total of 11 experimental data sets (Exp#1–11, Table S1), we inferred an average $k_{DMS+CH2OO} = (1.2 \pm 1.0)\times10^{-15}$ cm^3 s^{-1} (error bar is one standard deviation of the 11 data points).

3.2. Test of the effect of DMS photolysis

Although the absorption cross section of DMS is quite small (1.28×10^{-20} cm^2 at 248 nm and $<1\times10^{-22}$ cm^2 at 308 nm) (Limão-Vieira et al., 2002), yet the photolysis of DMS, especially at 248 nm, should be considered. We have performed a quantitative estimation of radical concentrations originating from the photolysis of DMS under the experimental conditions of this work (page S7) and show the results in Table S4.

In order to reduce the influence of DMS photolysis for the MVKO experiments, which require 248 nm photolysis (see Sect. 3.3), we constraint [DMS] $\leq 1.7\times10^{15}$ cm^{-3} and the laser fluence $I_{248nm} \leq 3.72$ mJ cm^{-2}. Then the amount of dissociated [DMS] would be $\leq 1\times10^{11}$ cm^{-3}, smaller than the dissociated $[CH_2I_2] \cong 1.2\times10^{12}$ cm^{-3} by an order of magnitude or more.

The expected products of DMS photolysis are CH_3 + CH_3S (Bain et al., 2018). Under the presence of O_2 (10 Torr), CH_3 would be converted into CH_3OO. These radicals (CH_3, CH_3OO, and CH_3S) are less reactive than I atoms or CIs. Thus, the small amount of dissociated [DMS] would only have a minor effect. And indeed, the results of CH_2OO+DMS reaction obtained with 248 nm photolysis (Figs. S2, S15, Table S2) are very similar to those with 308 nm photolysis (Figs. 2, S1, S12–S14, Table S1), indicating the effect of DMS photolysis is very minor. The values of $k_{DMS+CH2OO}$ obtained with 248 nm photolysis (Table S2) range from 1.6×10^{-15} to 3.2×10^{-15} cm^3 s^{-1}, which are only slightly higher than the results obtained with 308 nm photolysis (see Fig. S9). This indicates that the effect of the DMS photolysis would be on the order of $(1–3)\times10^{-15}$ cm^3 s^{-1} for $k_{DMS+CH2OO}$.

3.3. MVKO + DMS

Typical absorbance-time profiles of MVKO under various [DMS] ($\leq 1.3\times10^{15}$ cm^{-3}) are presented in Fig. 3. When generating MVKO via the reaction of $CH_3(C_2H_3)CI$ + O_2 at a high pressure like 300 Torr, the MVKO signal profiles rise slower than those of CH_2OO, with the maximum of the MVKO signal being at about 1.5 ms. Lin et al. have conducted detailed kinetic and quantum chemical studies on this phenomenon and concluded that the slow rise of the MVKO signal is due to the thermal decomposition of an adduct, $CH_3(C_2H_3)CIOO \rightarrow CH_3(C_2H_3)COO + I$ (Lin et al., 2020). See SI (Sect. S3, page S5) for details. This difference is consistent with the fact that MVKO is resonance-stabilized due to the extended conjugation of

its vinyl group (Barber et al., 2018) and thus the adduct $CH_3(C_2H_3)CIOO$ is relatively less stable due to disruption of the conjugation. Nevertheless, no significant changes in the absorbance-time profiles of MVKO with varying [DMS] can be noted (Fig. 3 inset), indicating the reaction of MVKO+DMS is insignificant. In Fig. 3, we can see that the lifetime of MVKO is on the order of 10 ms (i.e., a decay rate coefficient of ca. 100 s^{-1}) and the variation of the MVKO signal is insignificant upon adding [DMS]. This indicates that the reaction with DMS only changes, at the most, the MVKO lifetime by a small fraction (< 0.1) (a larger change would cause obvious deviation from the experimental observations of Fig. 3). Thus, $k_{DMS+MVKO}$ can be estimated to be on the order of $(100\ s^{-1})(0.1)/(1.3\times10^{15}\ cm^{-3}) \cong 10^{-14}\ cm^3\ s^{-1}$. Similar conclusion can be drawn from additional profiles recorded with different precursor concentrations and photolysis laser fluences and at different pressures (Fig. S16–S18).

To obtain more quantitative values of $k_{DMS+MVKO}$, we performed kinetic analysis and the details are given in SI (Sect. S3); selected results of k_{obs} as functions of [DMS] are presented in Fig. 4. Similar to the CH_2OO + DMS case, the rate coefficients for the reaction MVKO + DMS show no clear dependence on laser fluence or precursor concentration. From a total of 15 experiment sets (Exp#15–29, Table S3), we obtain an average rate coefficient $k_{DMS+MVKO} = (6.2 \pm 3.3)\times10^{-15}\ cm^3\ s^{-1}$ (error bar is one standard deviation of the 15 data points). As mentioned above, the MVKO precursor absorbs light weakly at 308 nm and requires 248 nm photolysis, such that small amounts of DMS would also be photodissociated. However, the above CH_2OO+DMS results indicate that the effect of DMS photolysis in our experiments is minor (on the order of $(1–3)\times10^{-15}\ cm^3\ s^{-1}$ for $k_{DMS+CH2OO}$), but may still lead to overestimation of $k_{DMS+MVKO}$. In this regard, the true value of $k_{DMS+MVKO}$ may be smaller than the above number.

3.4 Upper limiting rate coefficients and implications for atmospheric modelling

The experimental values of k_{DMS+CI} (Tables S1 and S3) are quite small, and their standard deviations are comparable to their average values, indicating that the measured k_{DMS+CI} are close to our detection limit. Here we choose the boundary of three standard deviations as the upper limits for k_{DMS+CI}, $k_{DMS+CH2OO} \le 4.2\times10^{-15}\ cm^3\ s^{-1}$ and $k_{DMS+MVKO} \le 1.6\times10^{-14}\ cm^3\ s^{-1}$ (Table 1). From Table 1, we can see that for the reactions of both CIs studied, the upper limits of the rate coefficients for their reactions with DMS, k_{DMS}, are much smaller than the literature values of their reactions with SO_2, k_{SO2}. The resulting ratios k_{DMS}/k_{SO2} are about four orders of magnitude smaller than that reported by Newland et al. (Newland et al., 2015)

The steady-state concentrations of CIs, $[CI]_{ss}$, in the troposphere have not been well established yet (Kim et al., 2015; Khan et al., 2018; Vereecken et al., 2017; Bonn et al., 2014; Boy et al., 2013). Novelli et al. have estimated an average CI concentration of 5×10^4 molecules cm^{-3} (with an order of magnitude uncertainty) for two environments they have investigated (Novelli et al., 2017). Due to fast thermal decomposition (Li et al., 2020; Smith et al., 2016; Vereecken et al., 2017; Stephenson and Lester, 2020) and/or fast reaction with water vapor (Chao et al., 2015; Lee, 2015; Osborn and Taatjes, 2015; Lin and Chao, 2017; Khan et al., 2018), $[CI]_{ss}$ is expected to be low, at least a couple of orders of magnitude lower than the steady-state concentration of OH radicals $[OH]_{ss}$. The small k_{DMS} values obtained in this work imply that these

reactions would not compete with the conventional DMS oxidation pathways like the reactions with OH or NO_3, of which both the reactant concentrations and rate coefficients are significantly larger. If the DMS reactions with CIs were to be competitive (e.g., 5% of the overall DMS removal) to those with NO_3 (e.g., $[NO_3] \cong 2.5\times10^8$ cm^{-3}) and OH (e.g., $[OH] \cong 1\times10^6$ cm^{-3}), the concentration of CIs would have to be unreasonably high, at the order of 10^{11} cm^{-3}.

Newland et al. performed their experiments on a mixture of 3 CIs (CH_2OO, MVKO, MACRO) as resulting from the ozonolysis of isoprene (Newland et al., 2015). The presence of these 3 CIs, however, cannot explain the four orders of magnitude difference to our results. Due to the lower yield of MACRO compared to the high yield for CH_2OO + MVKO (Nguyen et al., 2016; Zhang et al., 2002), it would require an unreasonably large $k_{DMS+MACRO}$, to explain the conclusion of Newland et al. In addition, the electronic structures of MACRO and MVKO are similar. Thus, similar reactivities are expected.

For the determination of the relative rate of the CI + DMS reaction, Newland et al. monitored the consumption of SO_2 over a measurement period of up to 60 min until approximately 25% of isoprene was consumed (Newland et al., 2015). Additional uncharacterized reaction pathways (e.g., reactions with the products) would lead to a bias in the inferred rate coefficients. A part of this high complexity of the isoprene-ozone-DMS-SO_2 system has been discussed by Newland et al. in the section of Experimental Uncertainties (Newland et al., 2015). Our direct measurements and kinetics are very straightforward; the obtained results for individual CIs may provide useful constraints for related ozonolysis systems.

3.5 Theoretical predictions for the reaction of CH_2OO + DMS

The potential energy surface for CH_2OO + DMS is shown in Figure 5. The reaction proceeds through a pre-reaction complex at –6.0 kcal mol^{-1} below the free reactants, from which a weakly bonded adduct, $(CH_3)_2SCH_2OO$ at an energy of –2.2 kcal mol^{-1}, can be formed through a submerged transition state (TS). At our level of theory, the wavefunction of this adduct converges to a closed-shell species with very strong zwitterionic character. A potential cycloadduct with a 4-membered –SCH_2OO– ring was found to be unstable. Two accessible product-forming transition states were discovered. The first channel starts from the pre-reaction complex, and leads to DMSO + CH_2O by direct transfer of the terminal O-atom of CH_2OO. A high barrier was found, 6.5 kcal mol^{-1} above the free reactants, leading to a slow reaction despite the predicted strong exothermicity of 79 kcal mol^{-1} for this channel. The second channel involves the migration of a DMS methyl H-atom to the outer oxygen of the $(CH_3)_2SCH_2OO$ adduct with a barrier of 4.7 kcal mol^{-1} above the free reactants, endothermically forming $CH_3S(=CH_2)CH_2OOH$ (*i.e.* the methylidene hydroperoxy equivalent of DMSO) with an energy 3.5 kcal mol^{-1} above the free reactants. No further low-lying reaction channels for this product were found, including formation of $C^{\bullet}H_2OOH$ + $CH_3SC^{\bullet}H_2$ which has an energy barrier of ≥ 20 kcal mol^{-1} at the M06-2X/cc-pVDZ level of theory. We did not examine more exotic CI reaction such as insertion in the DMS C–H bonds, as these are known to have comparatively high barriers (Decker et al., 2017). As described in the Supplement information, reaction with O_2 appears not competitive, as expected given that all intermediates are closed-shell (zwitterionic) species. For the reactions of DMS with substituted CI (*syn*-

CH_3CHOO and *anti*-CH_3CHOO; see Supplement information), we found similar complex stability but the adducts are energetically even less favorable, hampering their formation. For MVKO, the adduct was found to be unstable, and formation of DMSO, or H-migration of the DMS methyl hydrogen atoms has similar energy barriers as with CH_2OO. The most likely fate of the intermediates in the reaction of CI + DMS is thus reformation of the free reactants, with rapid equilibration between free reactants, pre-reaction complex, and adduct (where applicable). For CH_2OO + DMS, complex and adduct interconvert at rates > 10^7 s^{-1} at room temperature (> 4×10^6 s^{-1} at 200 K). The lifetime of the complex/adduct with respect to redissociation to the free reactants is estimated to be of the order of microseconds or less at room temperature, assuming a barrierless complexation channel.

The Supplement information also describes a set of calculations at a lower level of theory on the catalytic effect of DMS on a set of unimolecular and bimolecular loss processes of CI reactants. We conclude that DMS does not catalyze unimolecular decay of any of the CI examined, and that DMS does not enhance redissociation of the CI+SO_2 cycloadduct. No information is available on the impact of DMS on the forward reaction rates of CI bimolecular reactions. In the absence of catalytic effects, the observed elementary reaction of CI with DMS must occur through the pathways depicted in Figure 5. The total rate coefficient for product formation, i.e. DMSO or $CH_3S(=CH_2)CH_2OOH$, is predicted at:

$$k(298\ \mathrm{K}) = 5.5\times10^{-19}\ \mathrm{cm^3\ s^{-1}};$$

$$k(200\text{–}450\ \mathrm{K}) = 1.34\times10^{-44}\ T^{10.28}\ \exp(129\ \mathrm{K}/T)\ \mathrm{cm^3\ s^{-1}}.$$

Both channels contribute roughly equally at 298 K, with the higher TS being more loose, and the lower TS being more rigid. The $CH_3S(=CH_2)CH_2OOH$ product is intrinsically not very stable, and reverses to the $(CH_3)_2SCH_2OO$ adduct with a rate coefficient ≥ 10^{12} s^{-1}, over a very low reverse barrier of 1.3 kcal mol^{-1}. It seems unlikely that this product can undergo any bimolecular reactions prior to redissociation; reaction with O_2 was already found to be very slow. We should then consider that the only stable product effectively formed is DMSO + CH_2O, with the following rate coefficient:

$$k_{eff}(298\ \mathrm{K}) = 3.1\times10^{-19}\ \mathrm{cm^3\ s^{-1}};$$

$$k_{eff}(200\text{–}450\ \mathrm{K}) = 1.34\times10^{-26}\ T^{4.40}\ \exp(-2415\ \mathrm{K}/T)\ \mathrm{cm^3\ s^{-1}}.$$

These theoretical rate predictions are in full agreement with the experimental observations on the elementary reactions of CI with DMS. As documented in the Supplement information, similarly slow rate coefficients were predicted for substituted CIs, including MVKO formed in the ozonolysis of isoprene.

4 Summary

In this work, we present the first direct kinetic study of the reactions of DMS with CH_2OO and MVKO, which are the major CIs formed in the ozonolysis of isoprene. We generate the individual CIs by photolysis of the corresponding diiodo precursors in the presence of O_2 and monitored their decay via their strong UV absorption at 340 nm in real time. Our results do not indicate any notable reactivity of DMS with the two CIs studied. We therefore inferred the rate coefficients $k_{DMS+CH2OO} \le 4.2\times10^{-15}$ cm^3 s^{-1} and $k_{DMS+MVKO} \le 1.6\times10^{-14}$ cm^3 s^{-1}. For the reaction of CH_2OO + DMS, quantum chemistry

calculation did not find any low-energy reaction pathways, either by direct reaction or by catalysis of unimolecular reactions, and predicted an even smaller rate coefficient of $k_{DMS+CH2OO} = 3.1\times10^{-19}$ cm^3 s^{-1} at 298 K. Similarly low rate coefficients are predicted for substituted CIs such as CH_3CHOO and MVKO. Our results indicate that even in regions with high abundance of CIs and high concentrations of DMS, the isoprene-derived CIs will not notably contribute to the oxidation of DMS.

Supplement

The supplement related to this article is available online at: _____.

Author contributions

JJML conceived the experiment. MTK set up the experiment. MTK and IW performed the measurements. MTK analysed the experimental data. LV performed the theoretical calculations. MTK, IW, CF, LV, and JJML discussed the results and wrote the paper.

Competing interests

The authors declare that they have no conflict of interest.

Acknowledgements

This work is supported by Academia Sinica and Ministry of Science and Technology, Taiwan (MOST 106-2113-M-001-026-MY3; 108-2911-I-001-501(Orchid project)) and French Ministry of Europe and Foreign Affairs through the PHC Orchid project no. 40930 YC. LV is indebted to the Max Planck Graduate Center with the Johannes Gutenberg-Universität Mainz (MPGC), Germany.

References

Andreae, M. O., and Crutzen, P. J.: Atmospheric aerosols: biogeochemical sources and role in atmospheric chemistry, Science, 276, 1052-1058, https://doi.org/10.1126/science.276.5315.1052, 1997.

Atkinson, R., and Aschmann, S. M.: Hydroxyl radical production from the gas-phase reactions of ozone with a series of alkenes under atmospheric conditions, Environ. Sci. Technol., 27, 1357-1363, https://doi.org/10.1021/es00044a010, 1993.

Atkinson, R., Baulch, D. L., Cox, R. A., Crowley, J. N., Hampson, R. F., Hynes, R. G., Jenkin, M. E., Rossi, M. J., and Troe, J.: Evaluated kinetic and photochemical data for atmospheric chemistry: Volume I - gas phase reactions of O_x, HO_x, NO_x and SO_x species, Atmos. Chem. Phys., 4, 1461-1738, https://doi.org/10.5194/acp-4-1461-2004, 2004.

Atkinson, R., Baulch, D. L., Cox, R. A., Crowley, J. N., Hampson, R. F., Hynes, R. G., Jenkin, M. E., Rossi, M. J., Troe, J., and Wallington, T. J.: Evaluated kinetic and photochemical data for atmospheric chemistry: Volume IV – gas phase reactions of organic halogen species, Atmos. Chem. Phys., 8, 4141-4496, https://doi.org/10.5194/acp-8-4141-2008, 2008.

Bain, M., Hansen, C. S., and Ashfold, M. N. R.: Communication: Multi-mass velocity map imaging study of the ultraviolet photodissociation of dimethyl sulfide using single photon ionization and a PImMS2 sensor, J. Chem. Phys., 149, 081103, 10.1063/1.5048838, 2018.

Barber, V. P., Pandit, S., Green, A. M., Trongsiriwat, N., Walsh, P. J., Klippenstein, S. J., and Lester, M. I.: Four-Carbon Criegee Intermediate from Isoprene Ozonolysis: Methyl Vinyl Ketone Oxide Synthesis, Infrared Spectrum, and OH Production, J. Am. Chem. Soc., 140, 10866-10880, 10.1021/jacs.8b06010, 2018.

Beames, J. M., Liu, F., Lu, L., and Lester, M. I.: UV spectroscopic characterization of an alkyl substituted Criegee intermediate CH_3CHOO, J. Chem. Phys., 138, 244307, https://doi.org/10.1063/1.4810865, 2013.

Bell, R. D., and Wilson, A. K.: SO3 revisited: Impact of tight d augmented correlation consistent basis sets on atomization energy and structure, Chemical Physics Letters, 394, 105-109, https://doi.org/10.1016/j.cplett.2004.06.127, 2004.

Bonn, B., Bourtsoukidis, E., Sun, T. S., Bingemer, H., Rondo, L., Javed, U., Li, J., Axinte, R., Li, X., Brauers, T., Sonderfeld, H., Koppmann, R., Sogachev, A., Jacobi, S., and Spracklen, D. V.: The link between atmospheric radicals and newly formed particles at a spruce forest site in Germany, Atmos. Chem. Phys., 14, 10823-10843, https://doi.org/10.5194/acp-14-10823-2014W, 2014.

Boy, M., Mogensen, D., Smolander, S., Zhou, L., Nieminen, T., Paasonen, P., Plass-Dülmer, C., Sipilä, M., Petäjä, T., Mauldin, L., Berresheim, H., and Kulmala, M.: Oxidation of SO_2 by stabilized Criegee intermediate (sCI) radicals as a crucial source for atmospheric sulfuric acid concentrations, Atmos. Chem. Phys., 13, 3865-3879, https://doi.org/10.5194/acp-13-3865-2013, 2013.

Caravan, R. L., Vansco, M. F., Au, K., Khan, M. A. H., Li, Y.-L., Winiberg, F. A. F., Zuraski, K., Lin, Y.-H., Chao, W., Trongsiriwat, N., Walsh, P. J., Osborn, D. L., Percival, C. J., Lin, J. J.-M., Shallcross, D. E., Sheps, L., Klippenstein, S. J., Taatjes, C. A., and Lester, M. I.: Direct kinetic measurements and theoretical predictions of an isoprene-derived Criegee intermediate, Proc. Natl. Acad. Sci., 117, 9733-9740, 10.1073/pnas.1916711117, 2020.

Chang, Y.-P., Chang, C.-H., Takahashi, K., and Lin, J. J.-M.: Absolute UV absorption cross sections of dimethyl substituted Criegee intermediate $(CH_3)_2COO$, Chem. Phys. Lett., 653, 155-160, https://doi.org/10.1016/j.cplett.2016.04.082, 2016.

Chao, W., Hsieh, J.-T., Chang, C.-H., and Lin, J. J.-M.: Direct kinetic measurement of the reaction of the simplest Criegee intermediate with water vapor, Science, 347, 751, https://doi.org/10.1126/science.1261549, 2015.

Chao, W., Lin, Y.-H., Yin, C., Lin, W.-H., Takahashi, K., and Lin, J. J.-M.: Temperature and isotope effects in the reaction of CH_3CHOO with methanol, Phys. Chem. Chem. Phys., 21, 13633-13640, https://doi.org/10.1039/C9CP02534K, 2019.

Charlson, R. J., Lovelock, J. E., Andreae, M. O., and Warren, S. G.: Oceanic phytoplankton, atmospheric sulphur, cloud albedo and climate, Nature, 328, 655-661, https://doi.org/10.1038/326655a0, 1987.

Chhantyal-Pun, R., Davey, A., Shallcross, D. E., Percival, C. J., and Orr-Ewing, A. J.: A kinetic study of the CH_2OO Criegee intermediate self-reaction, reaction with SO_2 and unimolecular reaction using cavity ring-down spectroscopy, Phys. Chem. Chem. Phys., 17, 3617-3626, 10.1039/c4cp04198d, 2015.

Chhantyal-Pun, R., Shannon, R. J., Tew, D. P., Caravan, R. L., Duchi, M., Wong, C., Ingham, A., Feldman, C., McGillen, M. R., Khan, M. A. H., Antonov, I. O., Rotavera, B., Ramasesha, K., Osborn, D. L., Taatjes, C. A., Percival, C. J., Shallcross, D. E., and Orr-Ewing, A. J.: Experimental and computational studies of Criegee intermediate reactions with NH_3 and CH_3NH_2, Phys. Chem. Chem. Phys., 21, 14042-14052, https://doi.org/10.1039/C8CP06810K, 2019.

Cox, R. A., Ammann, M., Crowley, J. N., Herrmann, H., Jenkin, M. E., McNeill, V. F., Mellouki, A., Troe, J., and Wallington, T. J.: Evaluated kinetic and photochemical data for atmospheric chemistry: Volume VII - Criegee intermediates, Atmos. Chem. Phys. Discuss., 2020, 1-41, 10.5194/acp-2020-472, 2020.

Decker, Z. C. J., Au, K., Vereecken, L., and Sheps, L.: Direct experimental probing and theoretical analysis of the reaction between the simplest Criegee intermediate CH_2OO and isoprene, Phys. Chem. Chem. Phys., 19, 8541-8551, 10.1039/C6CP08602K, 2017.

Dunning, T. H.: Gaussian basis sets for use in correlated molecular calculations. I. The atoms boron through neon and hydrogen, J. Chem. Phys., 90, 1007-1023, 10.1063/1.456153, 1989.

Dunning, T. H., Peterson, K. A., and Wilson, A. K.: Gaussian basis sets for use in correlated molecular calculations. X. The atoms aluminum through argon revisited, J. Chem. Phys., 114, 9244-9253, 10.1063/1.1367373, 2001.

Eskola, A. J., Wojcik-Pastuszka, D., Ratajczak, E., and Timonen, R. S.: Kinetics of the reactions of CH_2Br and CH_2I radicals with molecular oxygen at atmospheric temperatures, Phys. Chem. Chem. Phys., 8, 1416-1424, https://doi.org/10.1039/B516291B, 2006.

Faloona, I.: Sulfur processing in the marine atmospheric boundary layer: A review and critical assessment of modeling uncertainties, Atmos. Environ., 43, 2841-2854, https://doi.org/10.1016/j.atmosenv.2009.02.043, 2009.

Foreman, E. S., Kapnas, K. M., and Murray, C.: Reactions between Criegee intermediates and the inorganic acids HCl and HNO_3: kinetics and atmospheric implications, Angew. Chem., Int. Ed., 55, 10419-10422, https://doi.org/10.1002/anie.201604662, 2016.

Frisch, M. J., Trucks, G. W., Schlegel, H. B., Scuseria, G. E., Robb, M. A., Cheeseman, J. R., Scalmani, G., Barone, V., Petersson, G. A., Nakatsuji, H., Li, X., Caricato, M., Marenich, A. V., Bloino, J., Janesko, B. G., Gomperts, R., Mennucci, B., Hratchian, H. P., Ortiz, J. V., Izmaylov, A. F., Sonnenberg, J. L., Williams, Ding, F., Lipparini, F., Egidi, F., Goings, J., Peng, B., Petrone, A., Henderson, T., Ranasinghe, D., Zakrzewski, V. G., Gao, J., Rega, N., Zheng, G., Liang, W., Hada, M., Ehara, M., Toyota, K., Fukuda, R., Hasegawa, J., Ishida, M., Nakajima, T., Honda, Y., Kitao, O., Nakai, H., Vreven, T., Throssell, K., Montgomery Jr., J. A., Peralta, J. E., Ogliaro, F., Bearpark, M. J., Heyd, J. J., Brothers, E. N., Kudin, K. N., Staroverov, V. N., Keith, T. A., Kobayashi, R., Normand, J., Raghavachari, K., Rendell, A.

P., Burant, J. C., Iyengar, S. S., Tomasi, J., Cossi, M., Millam, J. M., Klene, M., Adamo, C., Cammi, R., Ochterski, J. W., Martin, R. L., Morokuma, K., Farkas, O., Foresman, J. B., and Fox, D. J.: Gaussian 09 in, Wallingford, CT, 2009.

Gutbrod, R., Kraka, E., Schindler, R. N., and Cremer, D.: Kinetic and theoretical investigation of the gas-phase ozonolysis of isoprene: carbonyl oxides as an important source for OH radicals in the atmosphere, J. Am. Chem. Soc., 119, 7330-7342, https://doi.org/10.1021/ja970050c, 1997.

Hatakeyama, S., and Akimoto, H.: Reactions of criegee intermediates in the gas phase, Res. Chem. Intermed., 20, 503-524, 10.1163/156856794X00432, 1994.

Huang, H.-L., Chao, W., and Lin, J. J.-M.: Kinetics of a Criegee intermediate that would survive high humidity and may oxidize atmospheric SO_2, Proc. Natl. Acad. Sci., 112, 10857-10862, https://doi.org/10.1073/pnas.1513149112 2015.

Jardine, K., Yañez-Serrano, A. M., Williams, J., Kunert, N., Jardine, A., Taylor, T., Abrell, L., Artaxo, P., Guenther, A., Hewitt, C. N., House, E., Florentino, A. P., Manzi, A., Higuchi, N., Kesselmeier, J., Behrendt, T., Veres, P. R., Derstroff, B., Fuentes, J. D., Martin, S. T., and Andreae, M. O.: Dimethyl sulfide in the Amazon rain forest, Global Biogeochem. Cycles, 29, 19-32, https://doi.org/10.1002/2014GB004969, 2015.

Johnson, D., Lewin, A. G., and Marston, G.: The Effect of Criegee-Intermediate Scavengers on the OH Yield from the Reaction of Ozone with 2-methylbut-2-ene, J. Phys. Chem. A, 105, 2933-2935, 10.1021/jp003975e, 2001.

Johnson, D., and Marston, G.: The gas-phase ozonolysis of unsaturated volatile organic compounds in the troposphere, Chem. Soc. Rev., 37, 699-716, https://doi.org/10.1039/B704260B, 2008.

Khan, M. A. H., Percival, C. J., Caravan, R. L., Taatjes, C. A., and Shallcross, D. E.: Criegee intermediates and their impacts on the troposphere, Environmental Science: Processes & Impacts, 20, 437-453, 10.1039/C7EM00585G, 2018.

Kim, S., Guenther, A., Lefer, B., Flynn, J., Griffin, R., Rutter, A. P., Gong, L., and Cevik, B. K.: Potential role of stabilized Criegee radicals in sulfuric acid production in a high biogenic VOC environment, Environ. Sci. Technol., 49, 3383-3391, https://doi.org/10.1021/es505793t, 2015.

Lee, Y. P.: Perspective: Spectroscopy and kinetics of small gaseous Criegee intermediates, J. Chem. Phys., 143, 020901, https://doi.org/10.1063/1.4923165, 2015.

Lewis, T. R., Blitz, M. A., Heard, D. E., and Seakins, P. W.: Direct evidence for a substantive reaction between the Criegee intermediate, CH_2OO, and the water vapour dimer, Phys. Chem. Chem. Phys., 17, 4859-4863, https://doi.org/10.1039/C4CP04750H, 2015.

Li, Y.-L., Lin, Y.-H., Yin, C., Takahashi, K., Chiang, C.-Y., Chang, Y.-P., and Lin, J. J.-M.: Temperature-dependent rate coefficient for the reaction of CH_3SH with the simplest Criegee intermediate, J. Phys. Chem. A, 123, 4096-4103, https://doi.org/10.1021/acs.jpca.8b12553, 2019.

Li, Y.-L., Kuo, M.-T., and Lin, J. J.-M.: Unimolecular decomposition rates of a methyl-substituted Criegee intermediate syn-CH_3CHOO, RSC Advances, 10, 8518-8524, https://doi.org/10.1039/D0RA01406K, 2020.

Limão-Vieira, P., Eden, S., Kendall, P. A., Mason, N. J., and Hoffmann, S. V.: High resolution VUV photo-absorption cross-section for dimethylsulphide, $(CH3)_2S$, Chemical Physics Letters, 366, 343-349, https://doi.org/10.1016/S0009-2614(02)01651-2, 2002.

Lin, H.-Y., Huang, Y.-H., Wang, X., Bowman, J. M., Nishimura, Y., Witek, H. A., and Lee, Y.-P.: Infrared identification of the Criegee intermediates *syn*- and *anti*-CH_3CHOO, and their distinct conformation-dependent reactivity, Nat. Commun., 6, 7012, https://doi.org/10.1038/ncomms8012, 2015.

Lin, J. J.-M., and Chao, W.: Structure-dependent reactivity of Criegee intermediates studied with spectroscopic methods, Chem. Soc. Rev., 46, 7483-7497, https://doi.org/10.1039/C7CS00336F, 2017.

Lin, Y.-H., Takahashi, K., and Lin, J. J.-M.: Reactivity of Criegee intermediates toward carbon dioxide, J. Phys. Chem. Lett., 9, 184-188, https://doi.org/10.1021/acs.jpclett.7b03154, 2018.

Lin, Y.-H., Li, Y.-L., Chao, W., Takahashi, K., and Lin, J. J.-M.: The role of the iodine-atom adduct in the synthesis and kinetics of methyl vinyl ketone oxide—a resonance-stabilized Criegee intermediate, Phys. Chem. Chem. Phys., 22, 13603-13612, 10.1039/D0CP02085K, 2020.

Liu, F., Beames, J. M., Green, A. M., and Lester, M. I.: UV spectroscopic characterization of dimethyl- and ethyl-substituted carbonyl oxides, J. Phys. Chem. A, 118, 2298-2306, https://doi.org/10.1021/jp412726z, 2014a.

Liu, F., Beames, J. M., Petit, A. S., McCoy, A. B., and Lester, M. I.: Infrared-driven unimolecular reaction of CH_3CHOO Criegee intermediates to OH radical products, Science, 345, 1596-1598, 10.1126/science.1257158, 2014b.

Liu, Y., Bayes, K. D., and Sander, S. P.: Measuring Rate Constants for Reactions of the Simplest Criegee Intermediate (CH_2OO) by Monitoring the OH Radical, J. Phys. Chem. A, 118, 741-747, 10.1021/jp407058b, 2014c.

McCarthy, M. C., Cheng, L., Crabtree, K. N., Martinez, O., Nguyen, T. L., Womack, C. C., and Stanton, J. F.: The simplest Criegee intermediate ($H_2C{=}O{-}O$): isotopic spectroscopy, equilibrium structure, and possible formation from atmospheric lightning, J. Phys. Chem. Lett., 4, 4133-4139, https://doi.org/10.1021/jz4023128, 2013.

Meidan, D., Holloway, J. S., Edwards, P. M., Dubé, W. P., Middlebrook, A. M., Liao, J., Welti, A., Graus, M., Warneke, C., Ryerson, T. B., Pollack, I. B., Brown, S. S., and Rudich, Y.-. Role of Criegee intermediates in secondary sulfate aerosol formation in nocturnal power plant plumes in the southeast US, ACS Earth Space Chem., 3, 748-759, https://doi.org/10.1021/acsearthspacechem.8b00215, 2019.

Mir, Z. S., Lewis, T. R., Onel, L., Blitz, M. A., Seakins, P. W., and Stone, D.: CH_2OO Criegee intermediate UV absorption cross-sections and kinetics of CH_2OO + CH_2OO and CH_2OO + I as a function of pressure, Phys. Chem. Chem. Phys., 22, 9448-9459, 10.1039/D0CP00988A, 2020.

Nakajima, M., Yue, Q., and Endo, Y.: Fourier-transform microwave spectroscopy of an alkyl substituted Criegee intermediate *anti*-CH_3CHOO, J. Mol. Spectrosc., 310, 109-112, https://doi.org/10.1016/j.jms.2014.11.004, 2015.

Newland, M. J., Rickard, A. R., Vereecken, L., Muñoz, A., Ródenas, M., and Bloss, W. J.: Atmospheric isoprene ozonolysis: impacts of stabilised Criegee intermediate reactions with SO_2, H_2O and dimethyl sulfide, Atmos. Chem. Phys., 15, 9521-9536, https://doi.org/10.5194/acp-15-9521-2015, 2015.

Nguyen, T. B., Tyndall, G. S., Crounse, J. D., Teng, A. P., Bates, K. H., Schwantes, R. H., Coggon, M. M., Zhang, L., Feiner, P., Millller, D. O., Skog, K. M., Rivera-Rios, J. C., Dorris, M., Olson, K. F., Koss, A., Wild, R. J., Brown, S. S., Goldstein, A. H., de Gouw, J. A., Brune, W. H., Keutsch, F. N., Seinfeld, J. H., and Wennberg, P. O.: Atmospheric fates of Criegee intermediates in the ozonolysis of isoprene, Phys. Chem. Chem. Phys., 18, 10241-10254, https://doi.org/10.1039/C6CP00053C, 2016.

Novelli, A., Vereecken, L., Lelieveld, J., and Harder, H.: Direct observation of OH formation from stabilised Criegee intermediates, Phys. Chem. Chem. Phys., 16, 19941-19951, 10.1039/C4CP02719A, 2014.

Novelli, A., Hens, K., Tatum Ernest, C., Martinez, M., Nölscher, A. C., Sinha, V., Paasonen, P., Petäjä, T., Sipilä, M., Elste, T., Plass-Dülmer, C., Phillips, G. J., Kubistin, D., Williams, J., Vereecken, L., Lelieveld, J., and Harder, H.: Estimating the atmospheric concentration of Criegee intermediates and their possible interference in a FAGE-LIF instrument, Atmos. Chem. Phys., 17, 7807-7826, ttps://doi.org/10.5194/acp-17-7807-2017, 2017.

Osborn, D. L., and Taatjes, C. A.: The physical chemistry of Criegee intermediates in the gas phase, Int. Rev. Phys. Chem., 34, 309-360, 10.1080/0144235x.2015.1055676, 2015.

Percival, C. J., Welz, O., Eskola, A. J., Savee, J. D., Osborn, D. L., Topping, D. O., Lowe, D., Utembe, S. R., Bacak, A., M c Figgans, G., Cooke, M. C., Xiao, P., Archibald, A. T., Jenkin, M. E., Derwent, R. G., Riipinen, I., Mok, D. W. K., Lee, E. P. F., Dyke, J. M., Taatjes, C. A., and Shallcross, D. E.: Regional and global impacts of Criegee intermediates on atmospheric sulphuric acid concentrations and first steps of aerosol formation, Faraday Discuss., 165, 45-73, https://doi.org/10.1039/C3FD00048F, 2013.

Purvis, G. D., and Bartlett, R. J.: A full coupled-cluster singles and doubles model: The inclusion of disconnected triples, J. Chem. Phys., 76, 1910-1918, 10.1063/1.443164, 1982.

Sander, S. P., Abbat, J., Barker, J. R., Burkholder, J. B., Friedl, R. R., Golden, D. M., Huie, R. E., Kolb, C. E., Kurylo, M. J., Moortgat, G. K., Orkin, V. L., and Wine, P. H.: Chemical kinetics and photochemical data for use in atmospheric studies, Evaluation No. 17, in: hJPL Publication 10-6, Pasadena, 2011.

Sheps, L.: Absolute ultraviolet absorption spectrum of a Criegee intermediate CH_2OO, J. Phys. Chem. Lett., 4, 4201-4205, ttps://doi.org/10.1021/jz402191w, 2013.

Smith, M. C., Ting, W.-L., Chang, C.-H., Takahashi, K., Boering, K. A., and Lin, J. J.-M.: UV absorption spectrum of the C2 Criegee intermediate CH_3CHOO, J. Chem. Phys., 141, 074302, https://doi.org/10.1063/1.4892582, 2014.

Smith, M. C., Chao, W., Takahashi, K., Boering, K. A., and Lin, J. J.-M.: Unimolecular decomposition rate of the Criegee intermediate $(CH_3)_2COO$ measured directly with UV absorption spectroscopy, The Journal of Physical Chemistry A, 120, 4789-4798, https://doi.org/10.1021/acs.jpca.5b12124, 2016.

Stephenson, T. A., and Lester, M. I.: Unimolecular decay dynamics of Criegee intermediates: energy-resolved rates, thermal rates, and their atmospheric impact, Int. Rev. Phys. Chem., 39, 1-33, https://doi.org/10.1080/0144235X.2020.1688530, 2020.

Stone, D., Blitz, M., Daubney, L., Howes, N. U. M., and Seakins, P. W.: Kinetics of CH_2OO reactions with SO_2, NO_2, NO, H_2O and CH_3CHO as a function of pressure, Phys. Chem. Chem. Phys., 16, 1139-1149, https://doi.org/10.1039/C3CP54391A, 2014.

Su, M.-N., and Lin, J. J.-M.: Note: A transient absorption spectrometer using an ultra bright laser-driven light source, Rev. Sci. Instrum., 84, 086106, https://doi.org/10.1063/1.4818977, 2013.

Su, Y.-T., Huang, Y.-H., Witek, H. A., and Lee, Y.-P.: Infrared absorption spectrum of the simplest Criegee intermediate CH_2OO, Science, 340, 174-176, https://doi.org/10.1126/science.1234369, 2013.

Taatjes, C. A., Welz, O., Eskola, A. J., Savee, J. D., Osborn, D. L., Lee, E. P. F., Dyke, J. M., Mok, D. W. K., Shallcross, D. E., and Percival, C. J.: Direct measurement of Criegee intermediate (CH_2OO) reactions with acetone, acetaldehyde, and hexafluoroacetone, Phys. Chem. Chem. Phys., 14, 10391-10400, 10.1039/c2cp40294g, 2012.

Taatjes, C. A., Welz, O., Eskola, A. J., Savee, J. D., Scheer, A. M., Shallcross, D. E., Rotavera, B., Lee, E. P. F., Dyke, J. M., Mok, D. K. W., Osborn, D. L., and Percival, C. J.: Direct measurements of conformer-dependent reactivity of the Criegee intermediate CH_3CHOO, Science, 340, 177-180, https://doi.org/10.1126/science.1234689, 2013.

Ting, W.-L., Chen, Y.-H., Chao, W., Smith, M. C., and Lin, J. J.-M.: The UV absorption spectrum of the simplest Criegee intermediate CH_2OO, Phys. Chem. Chem. Phys., 16, 10438-10443, https://doi.org/10.1039/C4CP00877D, 2014.

Truhlar, D. G., Garrett, B. C., and Klippenstein, S. J.: Current Status of Transition-State Theory, The Journal of Physical Chemistry, 100, 12771-12800, 10.1021/jp953748q, 1996.

Vansco, M. F., Marchetti, B., and Lester, M. I.: Electronic spectroscopy of methyl vinyl ketone oxide: a four-carbon unsaturated Criegee intermediate from isoprene ozonolysis, J. Chem. Phys., 149, 244309, https://doi.org/10.1063/1.5064716, 2018.

Vansco, M. F., Marchetti, B., Trongsiriwat, N., Bhagde, T., Wang, G., Walsh, P. J., Klippenstein, S. J., and Lester, M. I.: Synthesis, electronic spectroscopy, and photochemistry of methacrolein oxide: a four-carbon unsaturated Criegee intermediate from isoprene ozonolysis, J. Am. Chem. Soc., 141, 15058-15069, https://doi.org/10.1021/jacs.9b05193, 2019.

Vereecken, L., Novelli, A., and Taraborrelli, D.: Unimolecular decay strongly limits the atmospheric impact of Criegee intermediates, Phys. Chem. Chem. Phys., 19, 31599-31612, 2017.

Wang, M. Y., Yao, L., Zheng, J., Wang, X., Chen, J. M., Yang, X., Worsnop, D. R., Donahue, N. M., and Wang, L.: Reactions of atmospheric particulate stabilized Criegee intermediates lead to high-molecular-weight aerosol components, Environ. Sci. Technol., 50, 5702-5710, https://doi.org/10.1021/acs.est.6b02114, 2016.

Welz, O., Savee, J. D., Osborn, D. L., Vasu, S. S., J., P. C., Shallcross, D. E., and Taatjes, C. A.: Direct kinetic measurements of Criegee intermediate CH_2OO formed by reaction of CH_2I with O_2, Science, 335, 204-204, https://doi.org/10.1126/science.1213229, 2012.

Welz, O., Eskola, A. J., Sheps, L., Rotavera, B., Savee, J. D., Scheer, A. M., Osborn, D. L., Lowe, D., Murray B., A., Xiao, P., Khan, M. A. H., Percival, C. J., Shallcross, D. E., and Taatjes, C. A.: Rate coefficients of C1 and C2 Criegee intermediate reactions with formic and acetic acid near the collision limit: direct kinetics measurements and atmospheric implications, Angew. Chem., Int. Ed., 53, 4547-4550, https://doi.org/10.1002/anie.201400964, 2014.

Yvon, S. A., Saltzman, E. S., Cooper, D. J., Bates, T. S., and Thompson, A. M.: Atmospheric sulfur cycling in the tropical Pacific marine boundary layer (12°S, 135°W): a comparison of field data and model results: 1. dimethylsulfide, J. Geophys. Res.: Atmos., 101, 6899-6909, https://doi.org/10.1029/95JD03356, 1996.

Zhang, D., Lei, W., and Zhang, R.: Machanism of OH formation from ozonolysis of isoprene: kinetics and product yield, Chem. Phys. Lett., 358, 171-179, https://doi.org/10.1016/S0009-2614(02)00260-9, 2002.

Zhao, Y., and Truhlar, D. G.: The M06 suite of density functionals for main group thermochemistry, thermochemical kinetics, noncovalent interactions, excited states, and transition elements: two new functionals and systematic testing of four M06-class functionals and 12 other functionals, Theor. Chem. Acc., 120, 215-241, 10.1007/s00214-007-0310-x, 2008.

Zhou, X., Liu, Y., Dong, W., and Yang, X.: Unimolecular reaction rate measurement of syn-CH_3CHOO, J. Phys. Chem. Lett., 10, 4817-4821, https://doi.org/10.1021/acs.jpclett.9b01740, 2019.

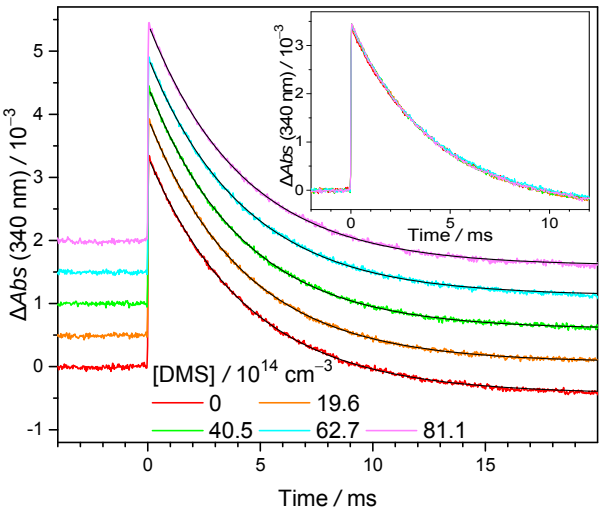

525

Figure 1: Representative time traces of CH_2OO absorption recorded at 340±5 nm under various [DMS]. The traces are shifted upward by various amounts for clearer visualization. Smooth black lines are the exponential fit. The photolysis laser (308 nm) pulse defines t = 0. The negative baseline (more obvious at long reaction time) is due to depletion of the precursor, CH_2I_2, which absorbs weakly at 340 nm ($\sigma = 8.33\times10^{-19}$ cm^2). (Atkinson et al., 2008) This depletion is constant in the probed time window and would not affect the kinetics of CH_2OO. Inset: The profiles without upshifting to show the overlapping. See Exp#1 of Table S1 for detailed experimental conditions.

530

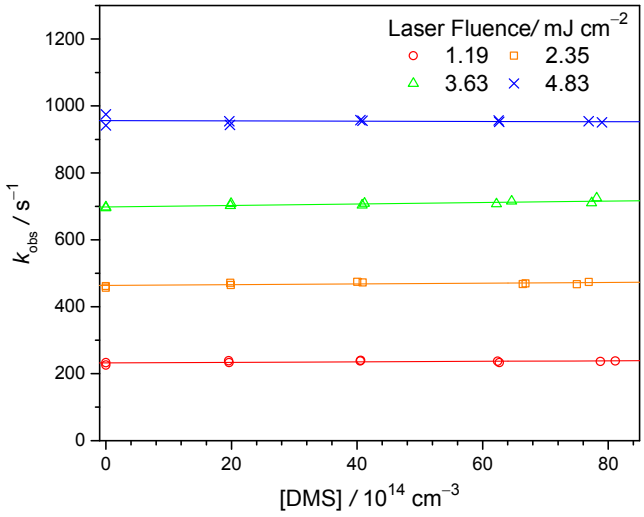

Figure 2: k_{obs} of CH_2OO against [DMS] determined from experiments (Exp#1–4, Table S1) at different photolysis laser fluences I_{308nm}; solid lines are linear fits. For each data point, the error of the single exponential fitting is lees than 1% (thus not shown).

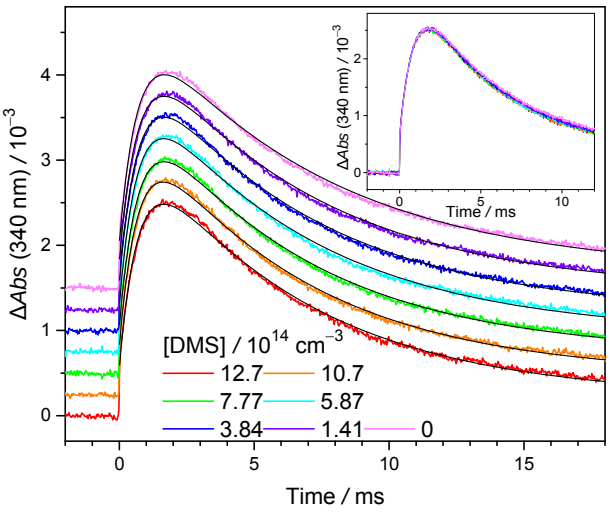

535

Figure 3: Representative MVKO absorbance-time profiles recorded at 340 nm under various [DMS] (298 K, 300 Torr, see Exp#16 of Table S3). The profiles are upshifted by various amounts to avoid overlapping. The color lines are experimental data and the smooth black lines are the model fit. Inset: The profiles without upshifting to show the overlapping.

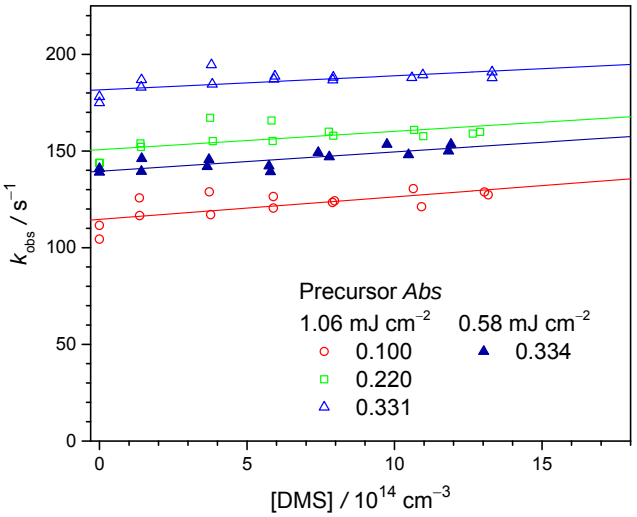

540 **Figure 4: Plot of the observed decay rate coefficient of MVKO k_{obs} against [DMS] at various laser fluences and precursor absorbances (Exp#15–18). For each data point, the fitting error bar is less than 1% (thus, not shown).**

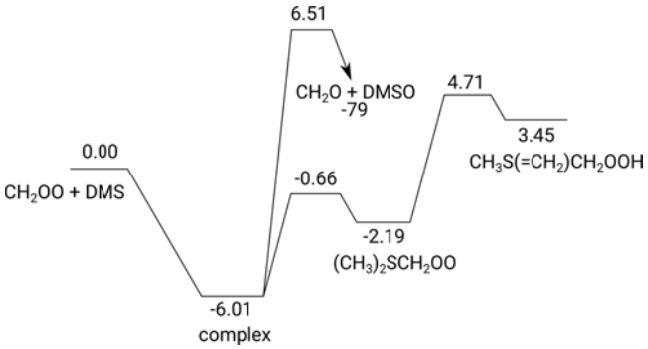

Figure 5: The potential energy surface of CH_2OO + DMS (kcal mol^{-1}), based on ZPE-corrected CCSD(T)//M06-2X relative energies.

Table 1: Summary of the bimolecular reaction rate coefficients of CI+SO_2 and CI+DMS.

CI	k_{DMS} / cm^3s^{-1}	k_{SO2} / cm^3s^{-1}	k_{DMS}/k_{SO2}	Reference
CH_2OO	< 4.2×10^{-15}	3.7×10^{-11}, [a]	< 1.1×10^{-4}	This work
MVKO	< 1.6×10^{-14}	4.1×10^{-11}, [b]	< 3.9×10^{-4}	This work
CIs	-	-	3.5±1.8	Newland et al. 2015

[a] The average value of $(3.4\pm0.4)\times10^{-11}$ (Stone et al., 2014), $(3.5\pm0.3)\times10^{-11}$ (Liu et al., 2014c), $(3.8\pm0.04)\times10^{-11}$ (Chhantyal-Pun et al., 2015), $(3.9\pm0.7)\times10^{-11}$ (Welz et al., 2012), and $(4.1\pm0.3)\times10^{-11}$ (Sheps, 2013).

[b] Caravan et al. 2020.

Supplementary Information for

Kinetics of Dimethyl Sulfide (DMS) Reactions with Isoprene-derived Criegee Intermediates Studied with Direct UV Absorption

Mei-Tsan Kuo,[1] Isabelle Weber,[2,6] Christa Fittschen,[2] Luc Vereecken[3,4], Jim Jr-Min Lin[1,5]

[1]Institute of Atomic and Molecular Sciences, Academia Sinica, Taipei 10617, Taiwan

[2]Univ. Lille, CNRS, UMR 8522 - PC2A - Physicochimie des Processus de Combustion et de l'Atmosphère, F-59000 Lille, France

[3]Max Planck Institute for Chemistry, Hahn-Meitner-Weg 1, 55128 Mainz, Germany

[4]Institute for Energy and Climate Research, IEK-8: Troposphere, Forschungszentrum Jülich GmbH, 52428 Jülich, Germany

[5]Department of Chemistry, National Taiwan University, Taipei 10617, Taiwan

[6]Present address: Department of Applied Chemistry and Institute of Molecular Science, National Chiao Tung University, Hsinchu 30010, Taiwan

ORCID:

Mei-Tsan Kuo: 0000-0002-7929-9265

Jim Jr-Min Lin: 0000-0002-8308-2552

Christa Fittschen: 0000-0003-0932-432X

Isabelle Weber: 0000-0001-5142-4557

Luc Vereecken: 0000-0001-7845-684X

S1 Summary of the experimental conditions and results

Table S1. Summary of the experimental conditions and results for the reaction CH_2OO+DMS at 308 nm photolysis. T = 296.8–297.2 K; $[O_2] = (3.28–3.32)\times10^{17}$ cm^{-3}; P_{total} = 299.9–301.5 Torr.

Exp#	$[CH_2I_2]$ /10^{13} cm^{-3}	I_{308nm} /mJ cm^{-2}	k_0 /s^{-1}	k_{DMS} /10^{-16} cm^3 s^{-1}
1	16.1	1.19	232±2[a]	7.8±4.1[a]
2	16.3	2.35	464±3	10.9±5.6
3	16.2	3.63	698±3	22.0±5.5
4	16.5	4.83	956±5	–4.1±10.4
5	12.6	0.34	54±2	9.1±4.5
6	21.2	0.31	79±2	10.2±4.1
7	20.7	0.31	90±2	8.6±4.9
8	21.1	0.74	188±1	–3.2±1.7
9	19.6	0.95	240±2	12.0±3.5
10	2.30	9.97	261±8	28.7±16.7
11	25.4	2.27	680±4	24.1±8.2
			average	11.5
			standard deviation[b]	10.3

[a] Averaged value ± 1 sigma error of the mean (statistical only, not including systematic errors). Note: 1 sigma error of the mean = standard deviation / sqrt(degrees of freedom)

[b] Standard deviation of the 11 data points of k_{DMS}.

Table S2. Summary of the experimental conditions and results for the reaction CH_2OO+DMS at 248 nm photolysis. T = 296.7K–296.8 K; $[O_2] = 3.29\times10^{17}$ cm^{-3}; P_{total} = 299.5–299.7 Torr.

Exp#	$[CH_2I_2]$ /10^{13} cm^{-3}	I_{248nm} /mJ cm^{-2}	k_0 /s^{-1}	k_{DMS} /10^{-16} cm^3 s^{-1}
12	19.3	1.10	109±1[a]	16.2±10.3[a]
13	19.0	2.18	197±1	25.5±8.6
14	18.9	3.17	275±1	31.6±11.5
			average	24.4
			standard deviation[b]	7.8

[a] Averaged value ± 1 sigma error of the mean (statistical only, not including systematic errors). Note: 1 sigma error of the mean = standard deviation / sqrt(degrees of freedom)

[b] Standard deviation of the 3 data points of k_{DMS}.

Table S3. Summary of the experimental conditions and results for the reaction MVKO + DMS at 248 nm photolysis. T = 297.0–298.1 K; $[O_2]$ = (3.28–3.41)×10^{17} cm^{-3}.

Exp#	Precursor Abs^b	P_{total} /Torr	I_{248nm} /mJ cm^{-2}	k_r /s^{-1}	adduct yield $1-\alpha^a$ /%	k_0 /s^{-1}	k_{DMS} /10^{-16} cm^3 s^{-1}
15	0.100	301.4	1.09	1182±14[b]	91.8±0.3[c]	115±2[b]	116.5±34.3[b]
16	0.220	303.0	1.06	1442±7	89.2±0.1	151±2	94.7±34.5
17	0.331	301.6	1.03	1641±5	87.2±0.1	182±2	73.2±24.0
18	0.334	301.9	0.58	1386±10	90.4±0.2	140±1	99.9±19.1
19	0.056	302.1	1.25	1033±48	91.1±1.6	123±8	75.0±70.7
20	0.151	302.2	1.23	1109±14	91.2±0.3	131±2	44.2±22.5
21	0.057	302.5	2.45	1203±14	90.6±0.2	146±2	19.6±17.0
22	0.158	302.3	2.43	1395±6	87.0±0.1	179±5	78.7±56.1
23	0.056	302.3	3.72	1330±5	88.9±0.3	229±2	33.2±15.9
24	0.160	302.4	3.67	1652±8	84.0±0.1	274±1	–15.0±16.7
25	0.179	30.6	1.19	1297±7	57.0±0.2	138±2	70.3±58.1
26	0.558	30.2	1.14	2123±19	49.2±0.1	255±2	67.8±59.3
27	0.289	100.2	1.18	1481±12	79.2±0.2	153±1	68.4±7.7
28	0.746	99.9	1.11	2146±8	70.7±0.1	321±2	39.6±25.8
29	0.142	299.5	1.19	1362±11	88.7±0.1	126±1	57.1±14.8
					average		61.6
					standard deviation[d]		33.4

[a] The yield of $CH_3(C_2H_3)ClOO$.

[b] The estimated absorbance of the precursor (1,3-diiodo-2-butene) at 238 nm in the photolysis reactor (using L = 426 cm).

[c] Averaged value ± 1 sigma error of the mean (statistical only, not including systematic errors). The actual error bar would be larger since k_r is highly correlated with other fitting parameters like $(1-\alpha)$. Lin et al. have used SO_2 scavenger to obtain more robust results for k_r (Lin et al., 2020).

[d] Standard deviation of the 15 data points of k_{DMS}.

S2 Observed decay rate coefficient of CH_2OO at various conditions

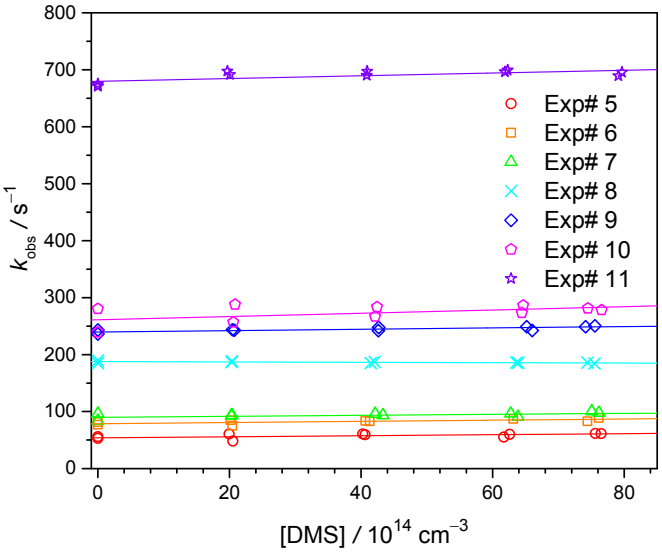

Fig. S1. First-order decay rate coefficient of CH_2OO, k_{obs}, against [DMS] at various experimental conditions (Exp#5–11, Table S1). The wavelength of the photolysis laser is 308 nm. For each data point, the error of the single exponential fitting is lees than 1% (thus not shown).

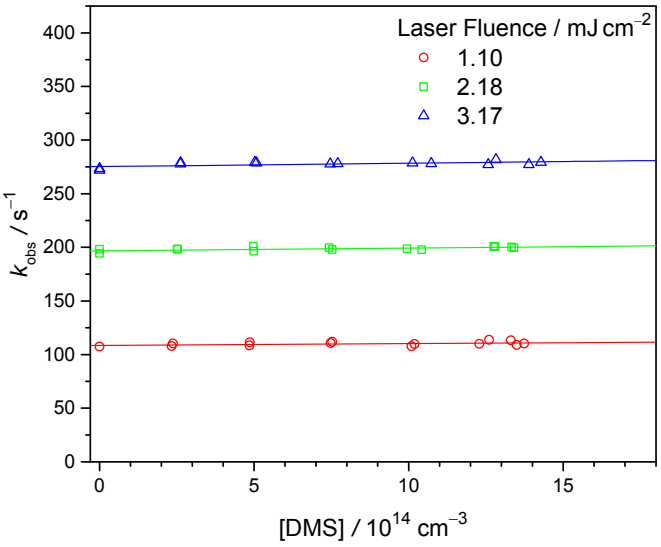

Fig. S2. First-order decay rate coefficient of CH_2OO, k_{obs}, against [DMS] at various photolysis laser fluence (Exp#12–14, Table S2). The wavelength of the photolysis laser is 248 nm. For each data point, the error of the single exponential fitting is lees than 1% (thus not shown).

S3 Kinetic model for MVKO reactions

To obtain more quantitative values for k_{DMS}, we performed kinetic analysis with the following model. At t = 0, the precursor ICH_2-CH=C(I)-CH_3 is photodissociated into $CH_3(C_2H_3)CI$ + I. Under the high $[O_2]$ conditions (~3.3×10^{17} cm^{-3}) in our experiment, the reactions of $CH_3(C_2H_3)CI + O_2$ (R3a) and (R3b) proceed within a very short time (< 0.1 ms). However, different from the case of CH_2OO, an additional MVKO signal rises slowly until about 2 ms (R3c), followed by a decay in longer reaction times (due to (R4) and (R5)). The formation/decomposition of the adduct of MVKO and I atom (R3b)/(R3c) are pressure dependent.

$CH_3(C_2H_3)CI + O_2 \rightarrow I + CH_3(C_2H_3)COO$ (MVKO) (R3a; αk_{O2})

$CH_3(C_2H_3)CI + O_2 + M \rightarrow CH_3(C_2H_3)CIOO + M$ (R3b; $(1-\alpha)k_{O2}$)

$CH_3(C_2H_3)CIOO + M \rightarrow I + CH_3(C_2H_3)COO + M$ (R3c; k_r)

$CH_3(C_2H_3)COO$ (MVKO) + DMS $\rightarrow$ Products (R4; k_{DMS})

$CH_3(C_2H_3)COO$ (MVKO) + X (radicals) $\rightarrow$ Products (R5; k_X)

The detail kinetics of the adduct decomposition into MVKO + I will be published elsewhere. In brief, MVKO is either formed directly (R3a), or via the formation and consecutive decomposition of an adduct of $CH_3(C_2H_3)CIOO$ ((R3b) and (R3c)). From the differential rate equations of these three reactions, the following analytical expression for [MVKO](t) can be derived:

$$\begin{aligned}[\mathrm{MVKO}](t) &= [\mathrm{MVKO}]_0 e^{-k_{\mathrm{obs}}t} + [\mathrm{adduct}]_0 \frac{k_r}{k_r - k_{\mathrm{obs}}}[e^{-k_{\mathrm{obs}}t} - e^{-k_r t}] \\ &= [\mathrm{MVKO}]_{\mathrm{total}}\{\alpha e^{-k_{\mathrm{obs}}t} + (1-\alpha)\frac{k_r}{k_r - k_{\mathrm{obs}}}[e^{-k_{\mathrm{obs}}t} - e^{-k_r t}]\}\end{aligned} \quad (3)$$

with α and $(1-\alpha)$ as the yields of the prompt MVKO and the adduct ($[MVKO]_{total}$ = $[MVKO]_0$ + $[adduct]_0$) and $k_{obs} = k_0 + k_{DMS}[DMS]$ as in the case of CH_2OO. Fitting this equation to the measured absorbance–time profiles treating k_{obs}, k_r, and α as variable parameters, we obtained k_{obs}. Selected results of k_{obs} are presented in Figure 4 and all results are summarized in Table S3.

S4 Observed decay rate coefficient of MVKO at various conditions

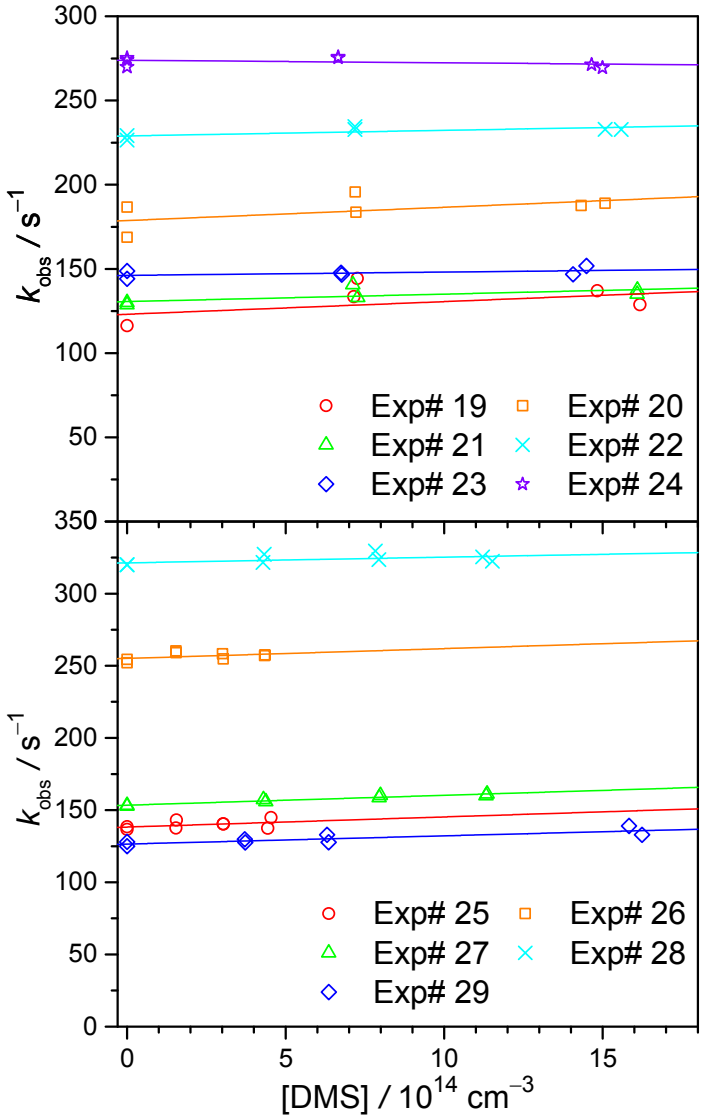

Fig. S3. First-order decay rate coefficient of MVKO, k_{obs}, against [DMS] at various experimental conditions (Exp#19–29). The wavelength of the photolysis laser is 248 nm.

S5 Effect of DMS photolysis

Assuming the photolysis yield of DMS is unity, the concentration of the photodissociated DMS, $[DMS]_{diss}$, can be deduced from the following equation:

$$[DMS]_{diss} = [DMS]\rho\sigma$$

$$\rho = I\frac{\lambda}{hc}$$

where $\rho = I\lambda/hc$ is the number of photons per unit area and σ is the reported absorption cross section of DMS(Limão-Vieira et al., 2002); I and λ are the fluence and wavelength of the photolysis laser; h and c are the Planck constant and speed of light, respectively. The maximum values of photodissociated DMS and CH_2I_2 precursor are estimated as in Table S4.

Table S4. Estimation for the photodissociated DMS and CH_2I_2.

Wavelength	I / mJ cm^{-2}	ρ / cm^{-2}	σ / cm^2	$[DMS]_{diss}/[DMS]$	[DMS] /cm^{-3}	$[DMS]_{diss}$ /cm^{-3}
248 nm	3.72	4.64×10^{15}	1.28×10^{-20}	5.9×10^{-5}	1.7×10^{15}	1.0×10^{11}
308 nm	9.97	1.55×10^{16}	$<1\times10^{-22}$	$<1.5\times10^{-6}$	8.1×10^{15}	$<1.3\times10^{10}$

				$[CH_2I_2]_{diss}/[CH_2I_2]$	$[CH_2I_2]$ /cm^{-3}	$[CH_2I_2]_{diss}$ /cm^{-3}
248 nm	3.17	3.96×10^{15}	1.6×10^{-18}	6.3×10^{-3}	1.9×10^{14}	1.2×10^{12}
308 nm	9.97	1.55×10^{16}	3.3×10^{-18}	5.1×10^{-2}	2.3×10^{13}	1.2×10^{12}

High $[DMS]_{diss}$ at 248 nm photolysis would generate radical products, which may react with CH_2OO or MVKO and may absorb light at our probe wavelength (see **Figure S4**). On the other hand, the very minor $[DMS]_{diss}$ at 308 nm photolysis would not cause a problem. Hence, at 248 nm photolysis, we limit [DMS] ≤ 1.7×10^{15} cm^{-3} and I_{248nm} ≤ 3.72 mJ cm^{-2} (Exp#23–24) to constraint $[DMS]_{diss}$ ≤ 1.0×10^{11} cm^{-3}. **Figure S5** shows the background trace at 248 nm photolysis with constraint [DMS] and I_{248nm}. No significant background due to $[DMS]_{diss}$ is observed, except absorption caused from the optics. Besides, in **Figure S9**, we can see that the results of CH_2OO+DMS reaction at 248 nm photolysis are quite similar to those at 308 nm, while a slightly higher k_{DMS} can be observed for 248 nm at high $I_{248\ nm}$, indicating that $[DMS]_{diss}$ only has a minor effect.

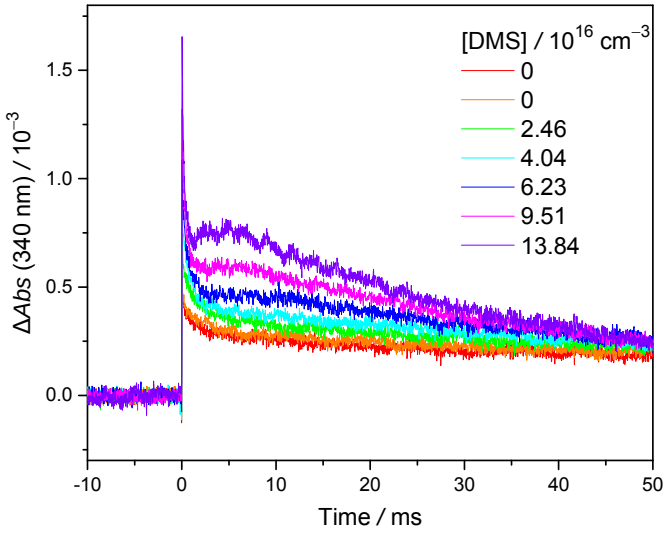

Fig. S4. Background traces recorded under extra-high [DMS]. The traces were obtained with 248 nm photolysis laser (I_{248nm} = 3.34 mJ cm^{-2}). The experimental conditions are : P_{total} =297.2 Torr, [O_2] =3.23 ×10^{17} cm^{-3}, T=299 K. The length of the cell for monitoring [DMS] is 1 cm. The photolysis laser pulse defines t = 0. The absorbance change under zero [DMS] comes from the interaction of the optics and the photolysis laser pulse, whereas the "spike" near time zero may come from the absorption of the radical products of DMS photolysis, likely CH_3S (Liu et al., 2005) and/or vibrationally excited CH_3S. Note that in the kinetic experiments, the used [DMS] was much lower (< 1.7×10^{15} cm^{-3}) such that the background did not depend on [DMS] (see Figure S5).

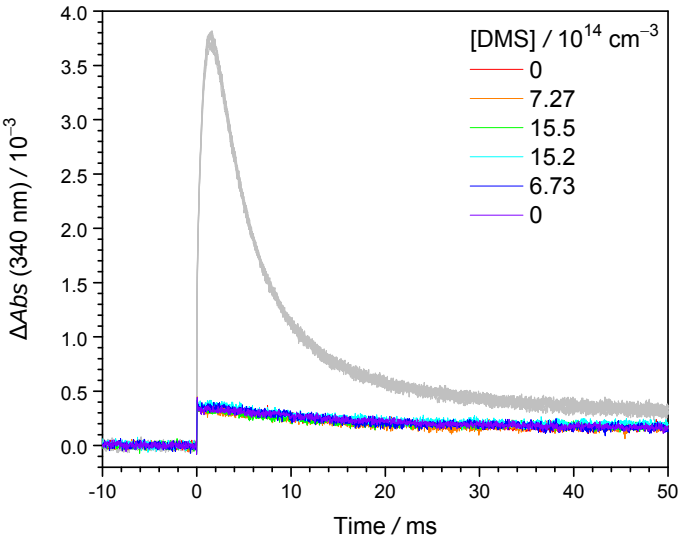

Fig. S5. Background traces under normal DMS concentrations, represented in colour lines, and the raw signal traces (without background subtraction), represented in grey

lines, obtained with 248 nm photolysis laser (I_{248nm} = 2.43 mJ cm^{-2}). See Exp#22 of Table S3 for the experimental conditions.

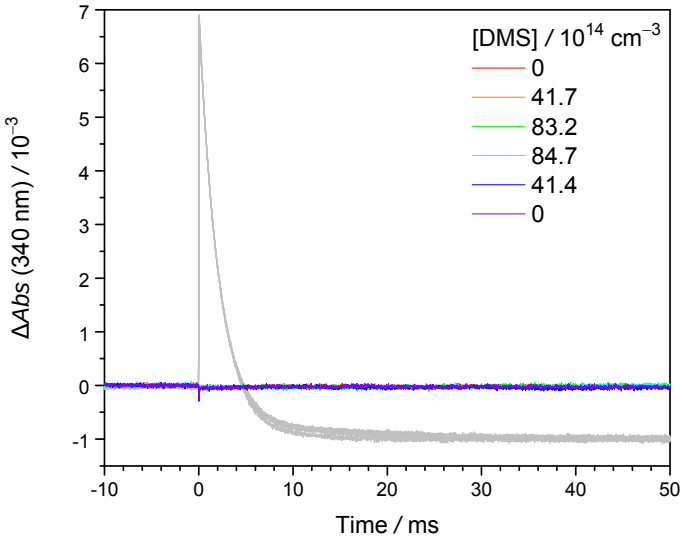

Fig. S6. Background traces under normal DMS concentrations, represented in colour lines, and the raw signal traces (without background subtraction), represented in grey lines, obtained with 308 nm photolysis laser (I_{308nm} = 2.35 mJ cm^{-2}). See Exp#2 of Table S1 for the experimental condition. Note that the optics (longpass filters) are different from those at 248 nm.

S6 Dependence of k_0 ,k_{DMS} , and k_r on laser fluence and precursor concentration

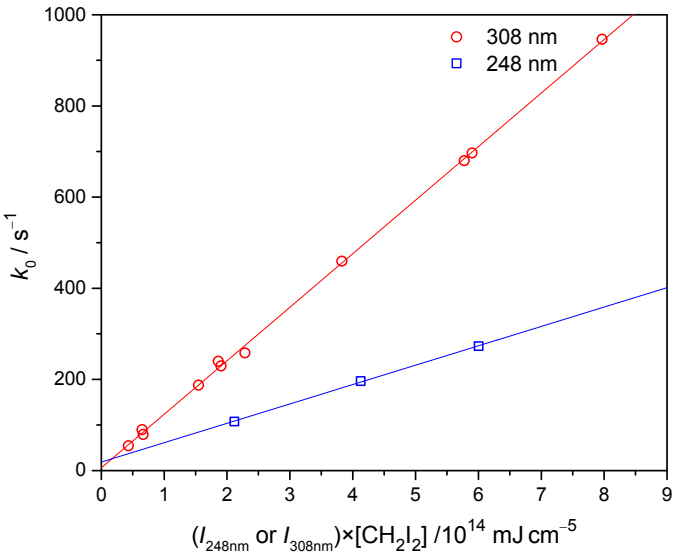

Fig. S7. Plot of k_0 against the product of the laser fluence (I_{248nm} or I_{308nm}) and the precursor concentration [CH_2I_2] for the experiments (Exp#1–14, Tables S1–S2) of CH_2OO+DMS reaction. The x-axis essentially represents the total amounts of radical species generated through the photolysis of the precursor (R1) and the subsequent reactions (R2). Higher radical concentration results in faster CH_2OO decay, thus higher k_0. The difference of the slopes mainly comes from the difference of CH_2I_2 absorption cross sections at these two wavelengths (see Table S4). The main loss processes of CH_2OO are reactions with radical byproducts like iodine atoms and its self-reaction. The observed values of k_0 (e.g., 232 s^{-1} for Exp#1) are consistent with the values (e.g., 180 s^{-1} at the condition of Exp#1) that are estimated using the reported kinetic data (yield and rate coefficients)(Mir et al., 2020;Ting et al., 2014). Note that there are experiments having different combinations of [CH_2I_2] and I_{308nm}, but very similar I_{308nm}×[CH_2I_2] (like Exp#3,11; Exp#1,9).

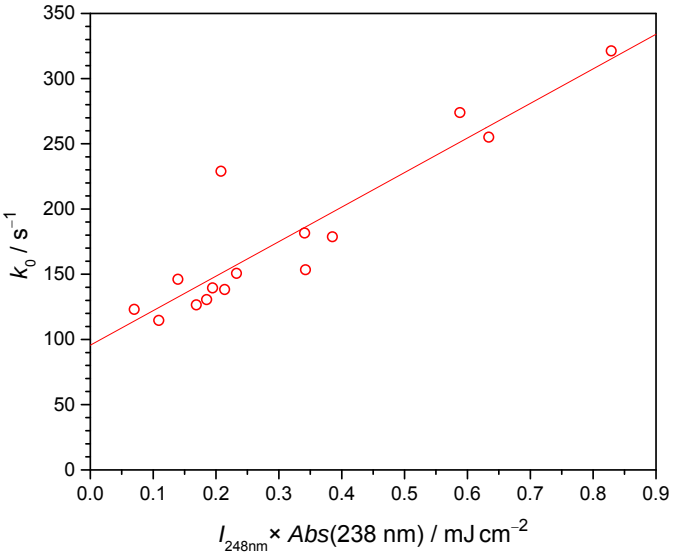

Fig. S8. As Figure S7, but for the experiments (Exp#15–29) of MVKO+DMS reaction. Because the absorption cross section of the precursor (1,3-diiodo-2-butene) is not available, we use the absorbance at 238 nm in the reactor (using L = 426 cm) to represent the concentration.

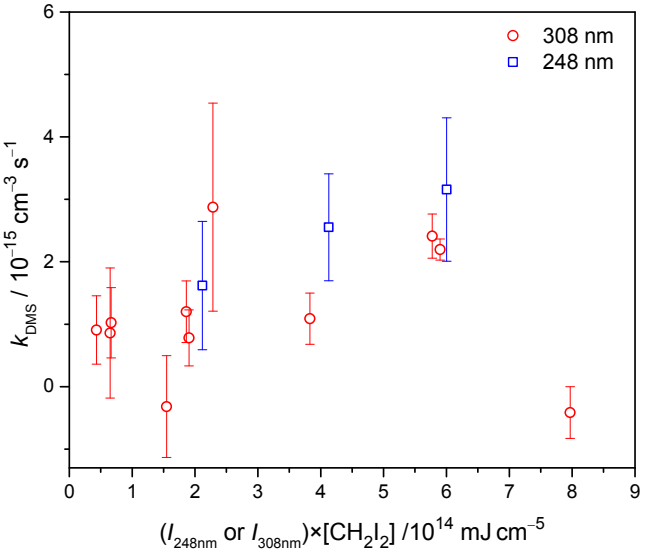

Fig. S9. Plot of k_{DMS} against the product of the laser fluence (I_{248nm} or I_{308nm}) and the precursor concentration [CH_2I_2] for the experiments (Exp#1–14, Tables S1–S2) of CH_2OO+DMS reaction. The x-axis essentially represents the total amounts of radical species generated through the photolysis of the precursor (R1) and the subsequent reactions (R2). No observable trend of k_{DMS} can be found for the data of 308 nm photolysis, whereas k_{DMS} at 248 nm photolysis increases as I_{248nm}x[CH_2I_2] increases, which may result from the increased

radical generation from the DMS photolysis. Note that there are experiments having different combinations of $[CH_2I_2]$ and I_{308nm}, but very similar I_{308nm}x$[CH_2I_2]$ (like Exp#3,11; Exp#1,9).

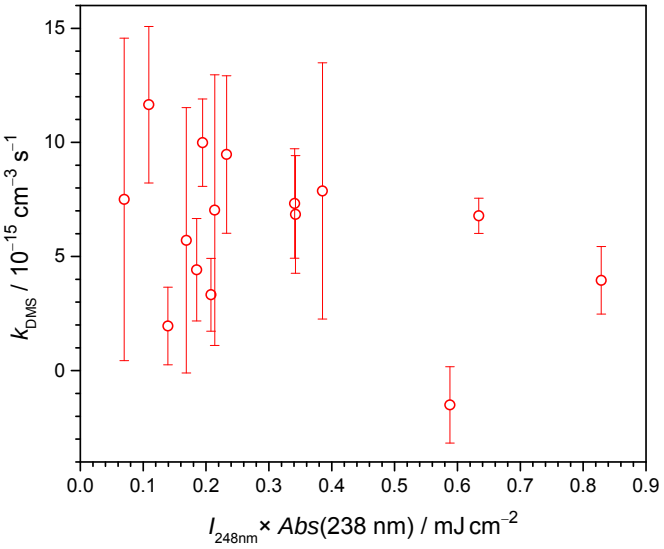

Fig. S10. As Figure S9, but for k_{DMS} in Exp#15–29 of MVKO+DMS reaction. No significant trend for k_{DMS} is observed. Because the absorption cross section of the precursor (1,3-diiodo-2-butene) is not available, we use the absorbance at 238 nm in the reactor (using L = 426 cm) to represent the concentration.

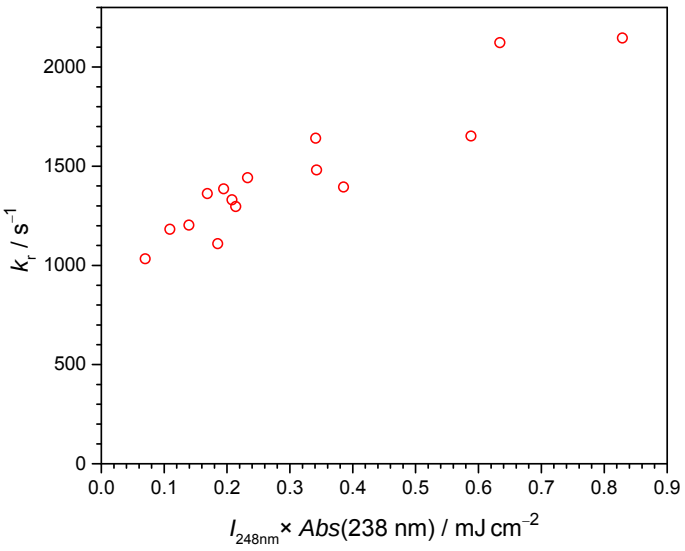

Fig. S11. Plot of k_r against the product of the laser fluence (I_{248nm}) and the absorbance of 1,3-diiodo-2-butene at 238 nm in the photolysis cell (*Abs*(238nm)) for the experiments of MVKO+DMS reaction (Exp#15–29, Tables S3). The x-axis essentially represents the total amounts of radical species generated through the photolysis of the precursor (R1) and the subsequent reactions (R2). Higher radical concentration results in faster decay of the adduct, thus higher k_r. Because the absorption cross section of the precursor (1,3-diiodo-2-butene) is not available, we use the absorbance at 238 nm in the reactor (using L = 426 cm) to represent the concentration.

S7 Representative time traces for the CH_2OO+DMS reaction obtained with 308 nm photolysis

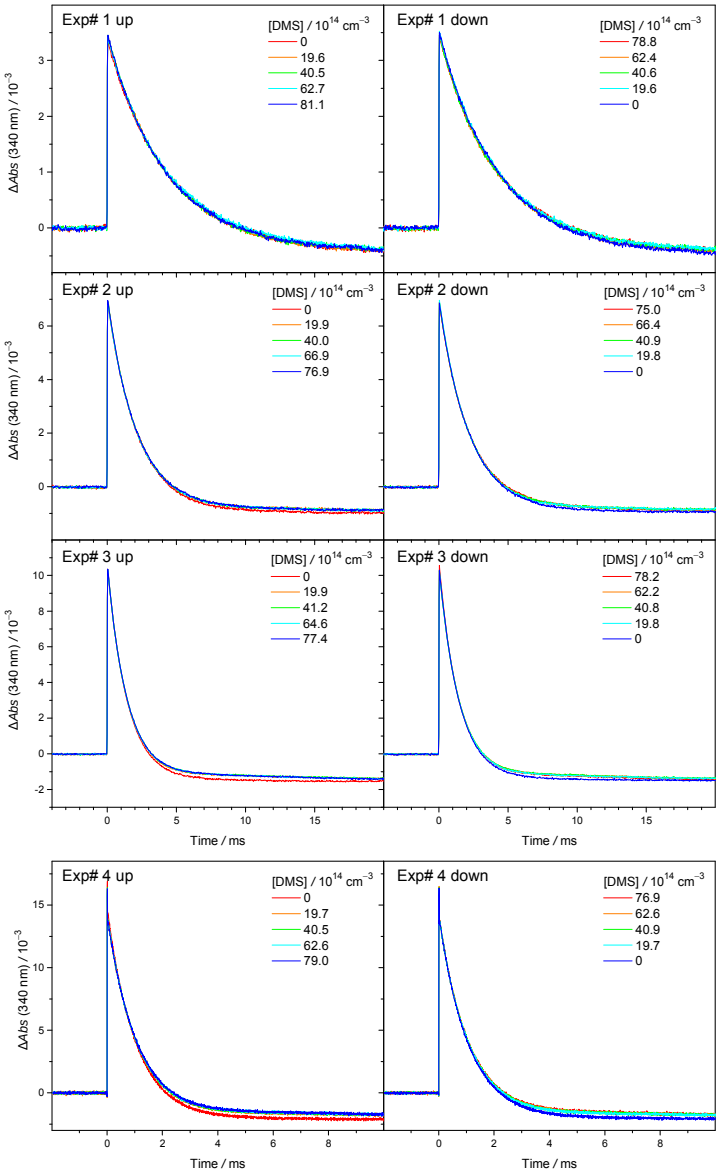

Fig. S12. Representative time traces of CH_2OO absorption at 340±5nm at various [DMS] (Exp#1–4). The wavelength of the photolysis laser was 308 nm and the laser pulse is set at the time zero. In each experiment, [DMS] was scanned from 0 to the maximum (labeled as "up"), and scanned from maximum to 0 (labeled as "down"). The negative baseline is resulted from the depletion of the precursor CH_2I_2.

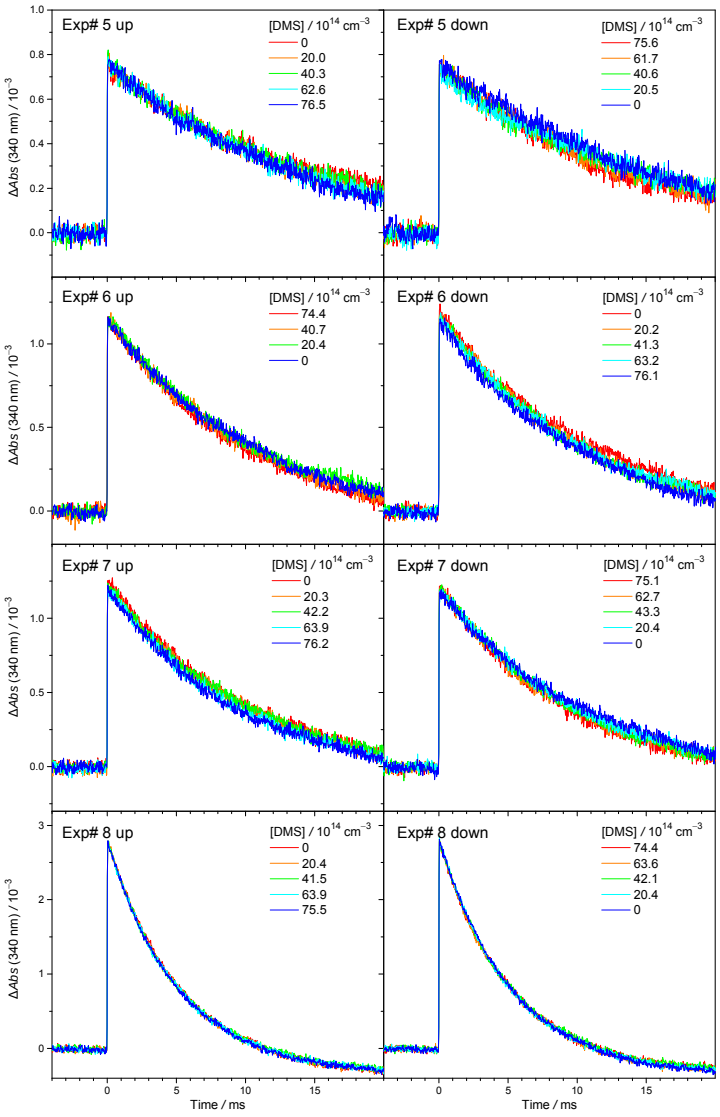

Fig. S13. As Fig. S12, but different experiment sets (Exp#5–8)

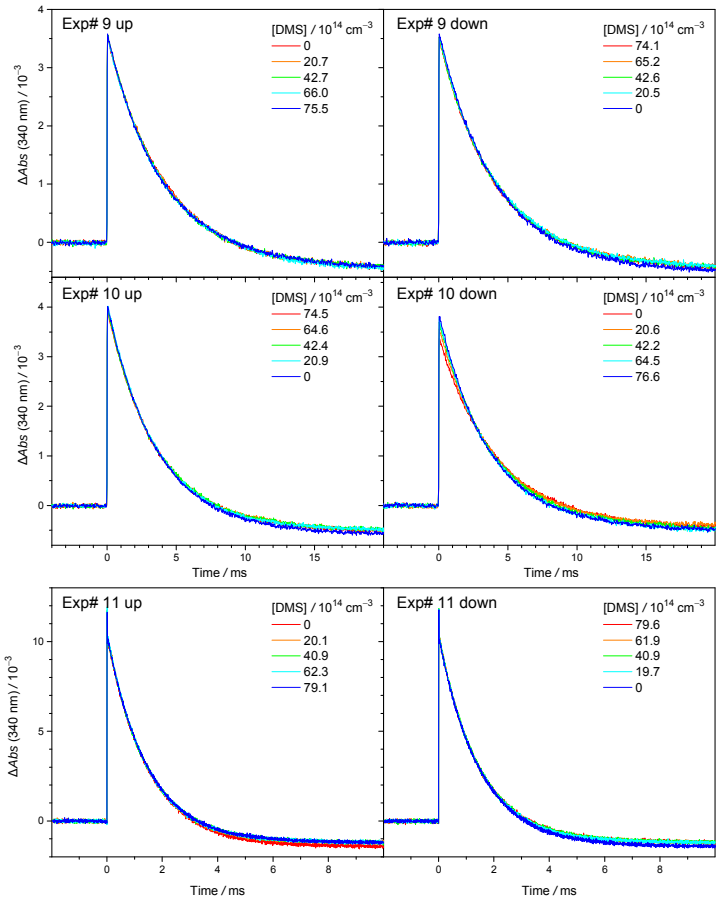

Fig. S14. As Fig. S12, but different experiment sets (Exp#9–11)

S8 Representative time traces for the CH_2OO+DMS reaction obtained with 248 nm photolysis

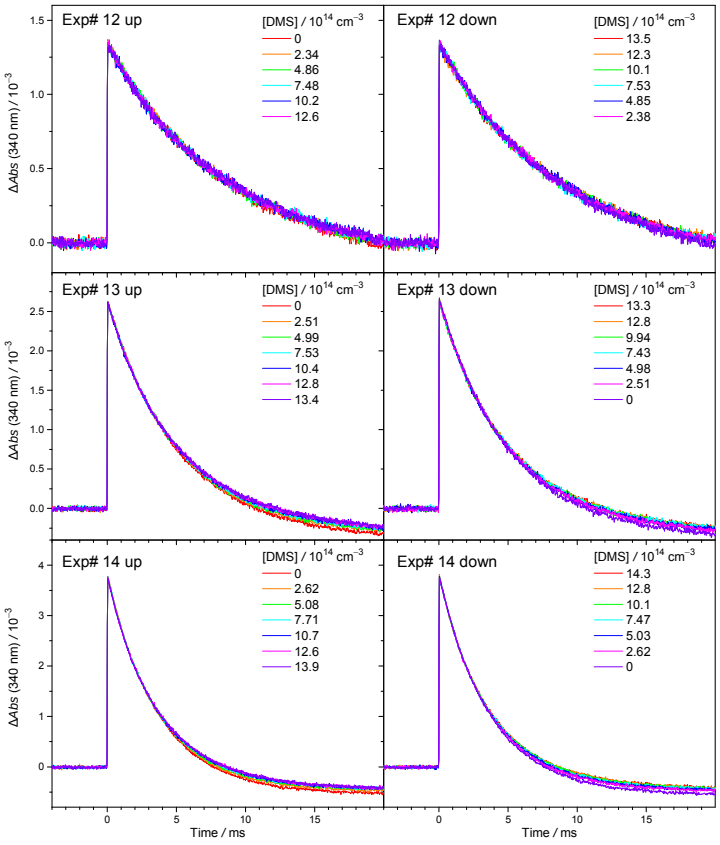

Fig. S15. Representative time traces of CH_2OO at 340±5nm at various [DMS] (Exp# 12–14). The wavelength of the photolysis laser was 248 nm and the laser pulse is set at the time zero. In each experiment, [DMS] was scanned from 0 to the maximum (labeled as "up"), and scanned from maximum to 0 (labeled as "down"). The negative baseline resulted from the depletion of the precursor CH_2I_2.

S9 Representative time traces for the MVKO+DMS reaction obtained with 248 nm photolysis

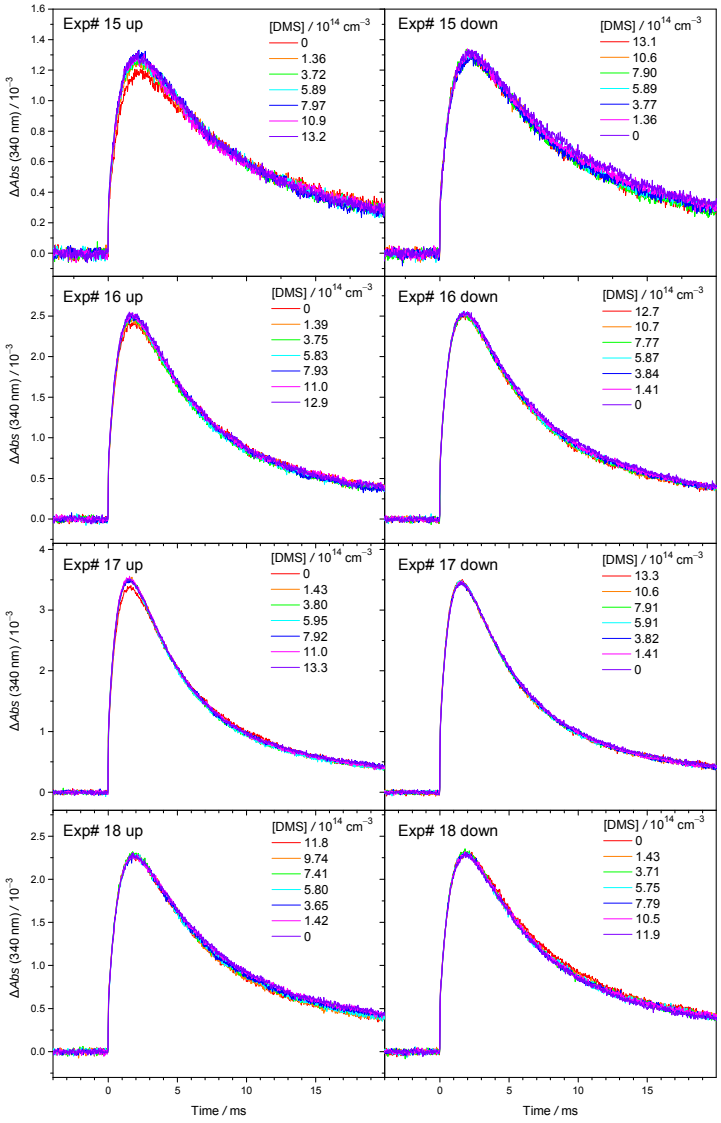

Fig. S16. Representative time traces of MVKO at 340±5nm at various [DMS] (Exp#15−18). The wavelength of the photolysis laser was 248 nm and the laser pulse is set at the time zero. In each experiment, [DMS] was scanned from 0 to the maximum (labeled as “up”), and scanned from maximum to 0 (labeled as “down”).

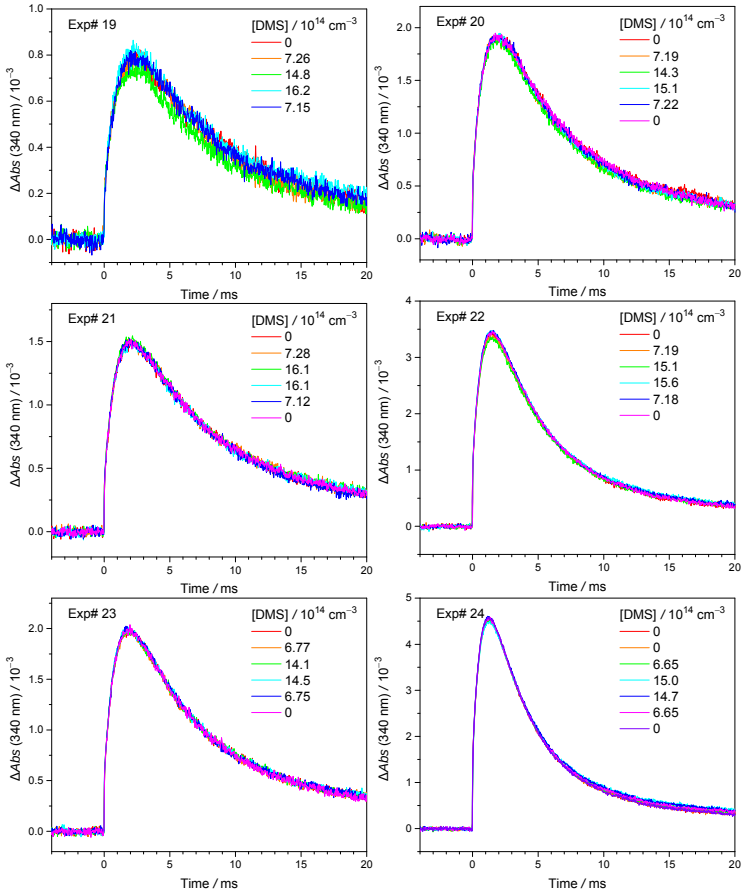

Fig. S17. Representative time traces of MVKO at 340±5nm at various [DMS] (Exp#19–24). The wavelength of the photolysis laser was 248 nm and the laser pulse is set at the time zero.

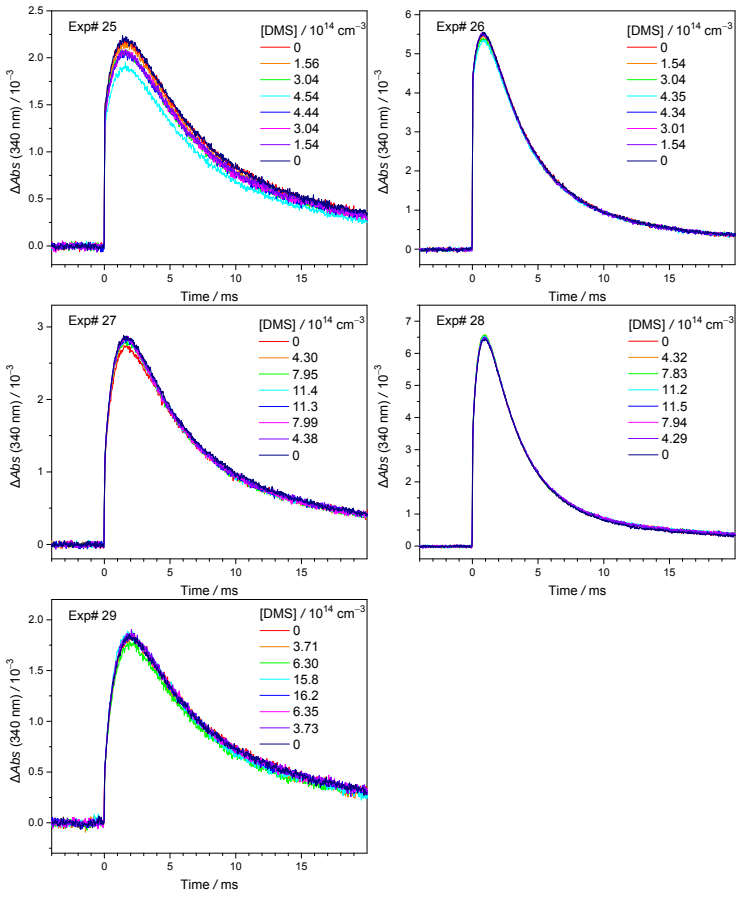

Fig. S18. As Fig. S17, but different experiment sets (Exp#25–29)

S10 Computational details for the reaction of CH_2OO + DMS

Additional methodological information

The CH_2OO + DMS system was characterized at the CCSD(T)/aug-cc-pVTZ//M06-2X/aug-cc-pV(T+d)Z level of theory. Though the computational demands of the reaction system prevent us from doing higher-level calculations at this time, this level of theory is expected to be sufficient to give a good idea of the PES layout, and derive rate coefficients with an accuracy of about one to two orders of magnitude. In particular, the study by Newland et al. proposes a very fast reaction which should then have a low energy barrier (Newland et al., 2015), whereas the current experimental study finds very slow elementary reactions which perforce must have a high energy barrier. The level of theory applied is able to easily discriminate between these extreme cases.

An additional set of exploratory calculations were performed at the M06-2X/cc-pVDZ level of theory, specifically on DMS + larger CI, DMS + CH_2OO in the presence of O_2, and unimolecular reactions of CH_2OO, *syn*-CH_3CHOO, *anti*-CH_3CHOO, and *cyc*-$CH_2OOS(O)O$- with and without complexation with DMS. These calculations at lower level are discussed here in the supporting information. For these calculations, only relative barrier heights on analogous reactions are important, which are sufficiently well described at the level of theory employed. As no indication for a significant enhancing effect on the reaction rate was found, no attempt was made to improve the absolute barrier height predictions.

Impact of substitutions of the CI, or the presence of O_2, on the CI + DMS reaction

Calculations for CH_2OO + DMS + O_2 reveal no influence of O_2 as a reaction partner, though the $(CH_3)_2SCH_2OO$ adduct may form a complex with O_2 stabilized by few kcal mol^{-1}. O_2 addition on the $(CH_3)_2SCH_2OO$ and $CH_3S(=CH_2)CH_2OOH$ adducts, forming triplet peroxy radicals, was found to have large barriers exceeding 15 kcal mol^{-1}, and is not competitive against redissociation of the CI+DMS adducts even at atmospheric O_2 concentrations.

Calculations on the reactions of *syn*-CH_3CHOO and *anti*-CH_3CHOO with DMS show that, as opposed to the CH_2OO case, formation of $(CH_3)_2SCH(CH_3)OO$ adducts is endothermic by a few kcal mol^{-1}, making reaction of substituted CI with DMS even less favorable. Finally, for all conformers of MVKO, the adduct with DMS was even found to be unstable at the M06-2X/cc-pVDZ level of theory: the needed C−S bond in the adduct appears to be too weak to compensate for the loss of conjugation stabilization in MVKO, and the system reverts to the MVKO + DMS complex instead, without a formal C−S bond. As a result, the barrier for the migration of a DMS methyl H-atom to the carbonyl oxide oxygen to form a methylidene adduct is ~10 kcal/mol higher than for the analogous TS in the CH_2OO+DMS system which does feature a weakly bonded intermediate adduct. The direct oxygen transfer from *E*- or *Z*-MVKO to DMS, forming MVK + DMSO, was found to have a similarly high energy barrier as in the CH_2OO+DMS system. No viable reaction channels were found

involving the double bond in MVKO. The lack of accessible transition states then prohibits rapid direct reaction between DMS and MVKO.

DMS as a catalyst

The experiments of Newland et al. found no evidence of DMS consumption (Newland et al., 2015), suggesting that the DMS activity hampering SO_2 oxidation by CI in their isoprene + O_3 system might be caused by catalytic effects. Hence, we examined whether the unimolecular decay of CI could be affected by complexation with DMS, performing a set of calculations using the lower level M06-2X/cc-pVDZ level of theory. At that level of theory, the complexes of CH_2OO, *syn*-CH_3CHOO and *anti*-CH_3CHOO with DMS are stabilized by 8.5 to 10.9 kcal mol^{-1} (likely overestimated due to basis set superposition errors). The barriers for dioxirane formation in CH_2OO, *syn*-CH_3CHOO and *anti*-CH_3CHOO are 22.0, 25.8 and 18.4 kcal mol^{-1} without DMS, respectively, while in the DMS complex they are 24.1, 26.8 and 20.4 kcal mol^{-1} above the complex, respectively. In *syn*-CH_3CHOO, the energy barrier for 1,4-H-migration (vinylhydroperoxide channel) without and with DMS are 12.7 and 15.8 kcal mol^{-1}, respectively, again calculated from the bottom of the CI-DMS complex. The dominant unimolecular reaction of *E*-MVKO is a 1,4-H-shift (VHP-channel), where at the M06-2X/cc-pVDZ level of theory, we find similar results as for the methylated CH_3CHOO, i.e. the barrier height without (12.1 kcal/mol) and with complexing DMS (14.2 kcal/mol from the ground state of the complex) are essentially identical (see Table S5). For *Z*-MVKO, the dominant unimolecular reaction is a 5-membered ring closure, and here too, DMS does not affect the intrinsic energy barrier for the reaction (see Table S5).

These results, despite being at a less reliable level of theory, strongly suggest that the DMS complexation does not lower the intrinsic barriers for unimolecular rearrangements, and might even slightly increase them. Any catalytic effect of DMS on the unimolecular decomposition of CI is then due to the energy release of the complexation, but this is insufficient to lower the decay TS close to or below the energy level of free CI + DMS, such that the main fate of the complex remains redissociation without chemical loss. For example, the net energy barrier for the DMS-catalysed *Z*-MVKO unimolecular reaction is ~ +4 kcal/mol, still implying a slow bimolecular reaction. This is in agreement with the observations of the current experimental study, which sees no enhanced CI loss in the presence of DMS.

There are many other reactions in the isoprene + O_3 system that might be catalytically enhanced or slowed by DMS, and examining all of these is outside the scope of this study. We did examine the reaction of DMS with the adduct of CH_2OO + SO_2, *i.e.* the thio-secondary ozonide (*cyc*-$CH_2OOS(O)O$-, thio-SOZ) (Kuwata et al., 2015;Vereecken et al., 2012) formed

prior to its decomposition to SO_3 + CH_2O. The DMS-catalyzed redissociation of thio-SOZ back to CH_2OO + SO_2, thus inhibiting SO_2 oxidation by CI, was found at the M06-2X/cc-pVDZ level of theory to have an energy barrier of 17.8 kcal mol^{-1}, too high to compete against SO_3 formation for which a barrier ≤ 10 kcal mol^{-1} was found (Kuwata et al., 2015). Any inhibiting effect by DMS on the CI + SO_2 reaction is thus not caused by an enhanced redissociation of the thio-SOZ intermediate.

No data is available elucidating whether bimolecular reactions of CI-DMS complexes with suitable co-reactants (SO_2, H_2O, acids,…), or alternatively DMS complexes of such co-reactants with free CI, are hindered or enhanced relative to those of the free CI + co-reactant.

Table S5: ZPE-corrected DMS complex energies, E(complex), and barrier heights E_b without and with a DMS complexing agent, at the M06-2X/cc-pVDZ level of theory. Energies are in kcal mol^{-1} and relative to the free reactants.

CI reaction	E_b	E(complex)	E_b(complex)
CH_2OO → cyc-CH_2OO-	22.0	–9.6	14.5
Z-CH_3CHOO → CH_2CHOOH	12.7	–8.6	7.2
Z-CH_3CHOO → cyc-$CH(CH_3)OO$-	25.8	–8.6	18.2
E-CH_3CHOO → cyc-$CH(CH_3)OO$-	18.4	–10.9	9.5
Z-$(CH=CH_2)C(CH_3)OO$ → cyc-CH-$CH_2C(CH_3)OO$-	12.1	–9.9	4.4
Z-$(CH=CH_2)C(CH_3)OO$ + DMS → MVK + DMSO	8.7		
E-$(CH_3)C(CH=CH_2)OO$ + DMS → MVK + DMSO	8.0		
$(CH_3)C(CH=CH_2)OO$ + DMS →$S(CH_3)(=CH_2)C(CH_3)(CH=CH_2)OOH$	11.2		

References

Kuwata, K. T., Guinn, E. J., Hermes, M. R., Fernandez, J. A., Mathison, J. M., and Huang, K.: A Computational Re-examination of the Criegee Intermediate–Sulfur Dioxide Reaction, J. Phys. Chem. A, 119, 10316-10335, 10.1021/acs.jpca.5b06565, 2015.

Limão-Vieira, P., Eden, S., Kendall, P. A., Mason, N. J., and Hoffmann, S. V.: High resolution VUV photo-absorption cross-section for dimethylsulphide, $(CH_3)_2S$, Chemical Physics Letters, 366, 343-349, https://doi.org/10.1016/S0009-2614(02)01651-2, 2002.

Lin, Y.-H., Li, Y.-L., Chao, W., Takahashi, K., and Lin, J. J.-M.: The role of the iodine-atom

adduct in the synthesis and kinetics of methyl vinyl ketone oxide—a resonance-stabilized Criegee intermediate, Phys. Chem. Chem. Phys., 22, 13603-13612, 10.1039/D0CP02085K, 2020.

Liu, C.-P., Reid, S. A., and Lee, Y.-P.: Two-color resonant four-wave mixing spectroscopy of highly predissociated levels in the $\tilde{A}^2A_1$ state of CH_3S, J. Chem. Phys., 122, 124313, 10.1063/1.1867333, 2005.

Mir, Z. S., Lewis, T. R., Onel, L., Blitz, M. A., Seakins, P. W., and Stone, D.: CH_2OO Criegee intermediate UV absorption cross-sections and kinetics of $CH_2OO + CH_2OO$ and $CH_2OO + I$ as a function of pressure, Phys. Chem. Chem. Phys., 22, 9448-9459, 10.1039/D0CP00988A, 2020.

Newland, M. J., Rickard, A. R., Vereecken, L., Muñoz, A., Ródenas, M., and Bloss, W. J.: Atmospheric isoprene ozonolysis: impacts of stabilised Criegee intermediate reactions with SO_2, H_2O and dimethyl sulfide, Atmos. Chem. Phys., 15, 9521-9536, 10.5194/acp-15-9521-2015, 2015.

Ting, W. L., Chang, C. H., Lee, Y. F., Matsui, H., Lee, Y. P., and Lin, J. J. M.: Detailed mechanism of the $CH_2I + O_2$ reaction: Yield and self-reaction of the simplest Criegee intermediate CH_2OO, J. Chem. Phys., 141, 104308, 10.1063/1.4894405, 2014.

Vereecken, L., Harder, H., and Novelli, A.: The reaction of Criegee intermediates with NO, RO_2, and SO_2, and their fate in the atmosphere, Phys. Chem. Chem. Phys., 14, 14682-14695, 10.1039/C2CP42300F, 2012.